IMMUNOLOGY

NLRC4 inflammasome–dependent cell death occurs by a complementary series of three death pathways and determines lethality in mice

Peipei Zhang[1†], Yifei Liu[2†], Lichen Hu[2], Kai Huang[2], Mao Hong[2], Yuze Wang[2], Xinrui Fan[2], Richard J. Ulevitch[3], Jiahuai Han[1,2*]

Inflammasome is an innate immune defense mechanism, but its overactivation can lead to host death. Here, we show that cell death dictates mouse death caused by NLRC4 inflammasome overactivation. To execute NLRC4-dependent cell death, three death pathways complement each other in a specific order: Pyroptosis pathway requiring caspase-1 and GSDMD is the default path; impairment of it initiates ASC-mediated caspase-8–dependent apoptosis; when these two pathways are blocked, caspase-1 triggers intrinsic apoptotic pathway. Blocking one or two of these death pathways inhibits induction of various cytokines and lipid mediators, but mice still succumb, and only genetic deletions that block all death paths prevent NLRC4-mediated cell death, tissue damage, and mice death. In addition, infection of nonpropagative *Salmonella*-caused mice death is attenuated by blocking these death pathways. Thus, to reduce the lethality of infection-related diseases, preventing cell death might be necessary when propagation of infected pathogen was controlled by other means.

INTRODUCTION

Inflammasomes are multiprotein complexes assembled by pattern recognition receptor (PRR) proteins in response to pathogen-associated molecular patterns and sterile stress signals (*1*). Canonical inflammasomes serve as key cellular activation platforms for caspase-1, whereas noncanonical inflammasomes elicit the activation of murine caspase-11 or human caspase-4 and caspase-5 (*2*–*4*). Activation of both types of inflammasomes leads to maturation of pro–interleukin-1β (IL-1β), pro–IL-18, and pyroptosis (*1*, *2*, *5*, *6*). Cleavage of gasdermin D (GSDMD) into N-terminal (N-GSDMD) and C-terminal (C-GSDMD) by caspase-1 is required for pyroptosis (*7*–*9*). The cleaved N-GSDMD fragment forms large oligomeric membrane pores that lead to pyroptosis, which facilitates IL-1β secretion (*10*, *11*). IL-1β and IL-18 secretions are part of the innate immune defense functions of inflammasomes, and pyroptosis could further enhance the release of these cytokines (*7*). Although "cytokine storm" is widely proposed to be responsible for the acute lethality of animal induced by systematic inflammation (*5*, *12*), inflammatory lipid mediators may also participate in the lethal inflammatory responses in vivo (*13*). It has been demonstrated that inflammasome-mediated cell death is important for controlling infected pathogens, and limiting pathogen(s) in vivo is critical for preventing host from mortality (*14*–*18*). However, hyperactivation of inflammasomes alone can also lead to organ damage and host death (*13*, *17*). The contribution of inflammasome-mediated cell death to animal death has remained unclear.

A canonical inflammasome complex is typically composed of a PRR protein, such as NLRP3 [NACHT, leucine-rich repeat, and pyrin domain (PYD)–containing protein 3], NLRP1, NLRC4 [NLR family caspase recruitment domain (CARD)–containing protein 4] or absent in melanoma-2 (AIM2) and pyrin, the adaptor protein ASC (apoptosis-associated speck-like protein), and caspase-1 (*1*, *19*). In the cases of NLRP3 and AIM2 inflammasomes, their interaction with caspase-1 is mediated by ASC, which interacts with NLRP3 or AIM2 through its PYD and with caspase-1 through its CARD. These proteins form structures known as "specks," where the activation and cleavage of caspase-1 occur (*1*, *19*). As for NLRC4 and murine NLRP1b that lack a PYD domain, specks can be formed by recruiting ASC directly through their CARD. Different from NLRP3 and AIM2, NLRC4 and NLRP1b can directly recruit caspase-1 via their CARD and activate caspase-1–mediated pyroptosis in an ASC-independent manner. However, specks formed with ASC still have promoting effects on the activation of NLRC4 and NLRP1b inflammasomes (*1*, *19*).

It was reported that genetic deletion of *Gsdmd* or *Caspase-1* (*Casp1*) blocked NLRP3 inflammasome–mediated pyroptosis, but cells still died via an apoptotic pathway (*7*, *20*, *21*). In this case, caspase-8 and ASC have been shown to be responsible for the apoptosis (*7*, *21*–*23*). Caspase-8 was also reported to compensate the loss of caspase-1 in NLRC4 inflammasome, and the $Rip3^{-/-}Casp1^{-/-}Casp8^{-/-}$ or $Asc^{-/-}Casp1^{-/-}Casp11^{-/-}$ mice were resistant to NLRC4-elicited hypothermia (*17*), which is known to often precede mouse death. A very recent report also showed flexible usage and switches of diverse cell death pathways in *Salmonella*-treated macrophages (*15*). To fully understand inflammasome-mediated cell death, we systematically studied switches from pyroptosis to apoptosis in canonical inflammasomes, including those inflammasomes where ASC is not obligatory. We showed that there are three cell death pathways that are adopted in a specific and preferential order downstream of inflammasome activation, and only blocking all of them can prevent cell death. We used flagellin-mediated NLRC4 inflammasome hyperactivation to evaluate whether and how cell death influences the outcome of mice. Strikingly, we found that as long as there is a remaining inflammasome-dependent cell death pathway, regardless of pyroptosis or apoptosis, the tissue/organ damages occur, and animals succumb. By this, we mean that it is

[1]State Key Laboratory of Cellular Stress Biology, Xiang'an Hospital of Xiamen University, Cancer Research Center of Xiamen University, School of Medicine, Xiamen University, Xiamen, Fujian 361102, China. [2]Research Unit of Cellular Stress of CAMS, School of Life Sciences, Xiamen University, Xiamen, Fujian 361102, China. [3]Department of Immunology and Microbiology, Scripps Research Institute, La Jolla, CA 92037, USA.
*Corresponding author. Email: jhan@xmu.edu.cn
†These authors contributed equally to this work.

cell death that plays a decisive role in the lethality of animals caused by inflammasome overactivation. In line with this result, impairment of the death pathways downstream of NLRC4 attenuated mice death caused by infection of nonpropagative *Salmonella*. These data suggest that blocking death pathways might be beneficial to the lethal infections when the propagation of pathogen(s) has been effectively inhibited by other therapeutic approaches.

RESULTS

The occurrence of cell death and subsequent cytolysis correlates with tissue damage and mouse death triggered by NLRC4 inflammasome

Flagellin is a subunit protein of bacterial flagellum. FlaTox, a combination of recombinant flagellin fused to the amino-terminal domain of *Bacillus anthracis* lethal factor (LFn-Fla) and anthrax protective antigen (PA), was developed to selectively activate NLRC4 (*13*). LFn-Fla can enter cells by PA-mediated endocytosis, leading to NLRC4-dependent pyroptosis, small intestinal damage, and mouse death (Fig. 1, A and B, and fig. S1, A to F) (*13*, *16*, *17*, *24*). Pyroptosis is a type of necrotic cell death with membrane disruption, which can be measured by lactate dehydrogenase (LDH) release. NLRC4-dependent pyroptosis and IL-1β release were detected in peritoneal lavage and blood of FlaTox-treated mice (fig. S1, G, H, K, and L). It was reported that extracellular flagellin induces tumor necrosis factor (TNF) and IL-6 production via an NLRC4-independent but Toll-like receptor 5 (TLR5)–dependent mechanism (*25*). As expected, *Nlrc4* deletion only slightly reduced the TNF and IL-6 levels in peritoneal lavage from FlaTox-treated mice (fig. S1, I and J). The levels of TNF and IL-6 in the blood of FlaTox-treated *Nlrc4*$^{-/-}$ mice were notable lower than those in wild-type (WT) mice (fig. S1, M and N). The LFn-Fla that we used can induce TNF and IL-6 production in bone marrow–derived macrophages independent of NLRC4 in the absence of PA (fig. S1, O to R). The local (peritoneal cavity) TNF and IL-6 should be induced by intraperitoneally injected FlaTox, and the circulating (blood) TNF and IL-6 ought to be controlled by other factor(s) that was directly or indirectly influenced by NLRC4 inflammasome activation.

Since caspase-1 and GSDMD are downstream of NLRC4 to mediate pyroptosis and the release of IL-1β and IL-18, we sought to examine the effect of *Gsdmd* and *Casp1* deletion in vivo. As we have *Casp1* and *Casp11* double knockout (KO) (*Casp1/11*$^{-/-}$) mice, and knowing that caspase-11 does not regulate FlaTox-induced NLRC4 inflammasome activation (*17*), we used *Casp1/11*$^{-/-}$ mice in our experiments. Slightly different from the published data on FlaTox-induced pathology and body temperature drop (*17*), *Gsdmd*$^{-/-}$ and *Casp1/11*$^{-/-}$ mice behaved more like WT mice in FlaTox-induced small intestinal damage and death (Fig. 1, A and B). It is known that deletion of *Gsdmd* or *Casp1* blocks pyroptosis as well as IL-1β and IL-18 release (*1*, *7*–*9*), but we found that their deletion is quite different from *Nlrc4* deletion, which totally blocks FlaTox-induced mouse death (Fig. 1, A and B). Thus, a more complicated mechanism is underneath the in vivo responses to FlaTox.

To address the mechanism of in vivo responses to FlaTox, we analyzed FlaTox-induced pyroptosis ex vivo. We collected peritoneal lavages at 1 and 2 hours after FlaTox injection and measured the release of LDH, IL-1β, TNF, and IL-6. Deletion of *Gsdmd* or *Casp1* effectively blocked LDH release at 1 hour. However, the level of LDH release into peritoneal cavity became comparable among *Gsdmd*$^{-/-}$, *Casp1*$^{-/-}$, and WT mice at later times (Fig. 1C), indicating that cytolysis still occurred. It is known that in cultured cells, pyroptotic stimuli can trigger apoptosis when *Casp1* or *Gsdmd* was deleted (*7*, *20*, *21*). Therefore, LDH release in *Gsdmd*$^{-/-}$, *Casp1*$^{-/-}$ mice at later times could be attributed to secondary necrotic lysis of the apoptotic cells or caspase-3–mediated pyroptosis via GSDME cleavage (*26*, *27*). However, the latter hypothesis is unlikely as no difference was observed between *Gsdmd*$^{-/-}$ mice and *Gsdmd*$^{-/-}$*Gsdme*$^{-/-}$ mice (fig. S2, A to H). IL-1β secretion into peritoneal cavity was inhibited to different extents by deletion of *Gsdmd*$^{-/-}$ or *Casp1*$^{-/-}$ at 1 hour, and continued inhibition was observed in *Casp1*$^{-/-}$ but not *Gsdmd*$^{-/-}$ mice (Fig. 1D). The blockade of IL-1β release in *Casp1*$^{-/-}$ mice should be resulted from failure to process IL-1β to its mature form (*28*), and the inhibited IL-1β release did not reduce animal death, supporting the conclusion by a previous report that flagellin-induced mouse death is independent of IL-1β and IL-18 production (*13*). The release of TNF and IL-6 into peritoneal cavity was not affected by gene deletion of *Gsdmd* or *Casp1* (Fig. 1, E and F) because FlaTox-induced TNF and IL-6 production is NLRC4 pathway independent (Fig. 1, E and F). We then analyzed blood from FlaTox-treated mice and found that deletion of *Gsdmd* did not affect the increase of circulating LDH, IL-1β, TNF, and IL-6, and the *Casp1* deletion also had no effect except for affecting IL-1β release (fig. S1, S to V). By measuring the correlations, we observed that the increase of blood TNF and IL-6 in FlaTox-treated mice is associated with LDH release but not IL-1β release. Here, it should be noted that TNF is not required for the death of FlaTox-treated mice as FlaTox was equally toxic to WT and *Tnfr1*$^{-/-}$ mice (fig. S1W).

Since inflammatory signaling lipids such as prostaglandins and leukotrienes are known to play a role in inflammasome-mediated pathological effects, we measured representatives of these lipids in peritoneal lavages at 0, 20, and 60 min after FlaTox injection. The induction of the eicosanoid lipids generated by lipoxygenase was almost completely blocked in both *Gsdmd*$^{-/-}$ and *Casp1/11*$^{-/-}$ mice (Fig. 1G). Some of the cyclooxygenase (COX)–produced eicosanoids, prostaglandin D_2 (PGD_2), and thromboxane B2 (TXB_2) were significantly inhibited in *Gsdmd*$^{-/-}$ and *Casp1/11*$^{-/-}$ mice, whereas the inhibition was slight on the production of prostaglandin E_2 (PGE_2) (Fig. 1H). We used COX inhibitor SC-560, which effectively inhibited the increase of PGE_2 and TXB_2 and, to a less extent, of PGD_2 in peritoneal lavages of FlaTox-treated mice (Fig. 1I), and had little or no effect on the other lipids (Fig. 1J). FlaTox-induced death of mice was not affected by SC-560 (Fig. 1K). Thus, none of these eicosanoid lipids is required for the lethality of FlaTox-treated mice (Fig. 1, A and G to K). Collectively, as for FlaTox-induced mouse death per se, TNF, IL-1β/18 induction, and "eicosanoid storm" seem to be dispensable, and only LDH release was found to have correlation with FlaTox-induced mouse death. Thus, cytolysis in vivo is likely the major risk of animal death.

Cell death driven by NLRC4 and other canonical inflammasomes could be mediated by apoptosis when pyroptosis was blocked

To understand why LDH release still occurred when pyroptotic pathway was already blocked in FlaTox-treated mice, we explored possible switches in death pathways. It was reported that ASC in NLRP3 or AIM2 complex can recruit caspase-8 to trigger apoptosis

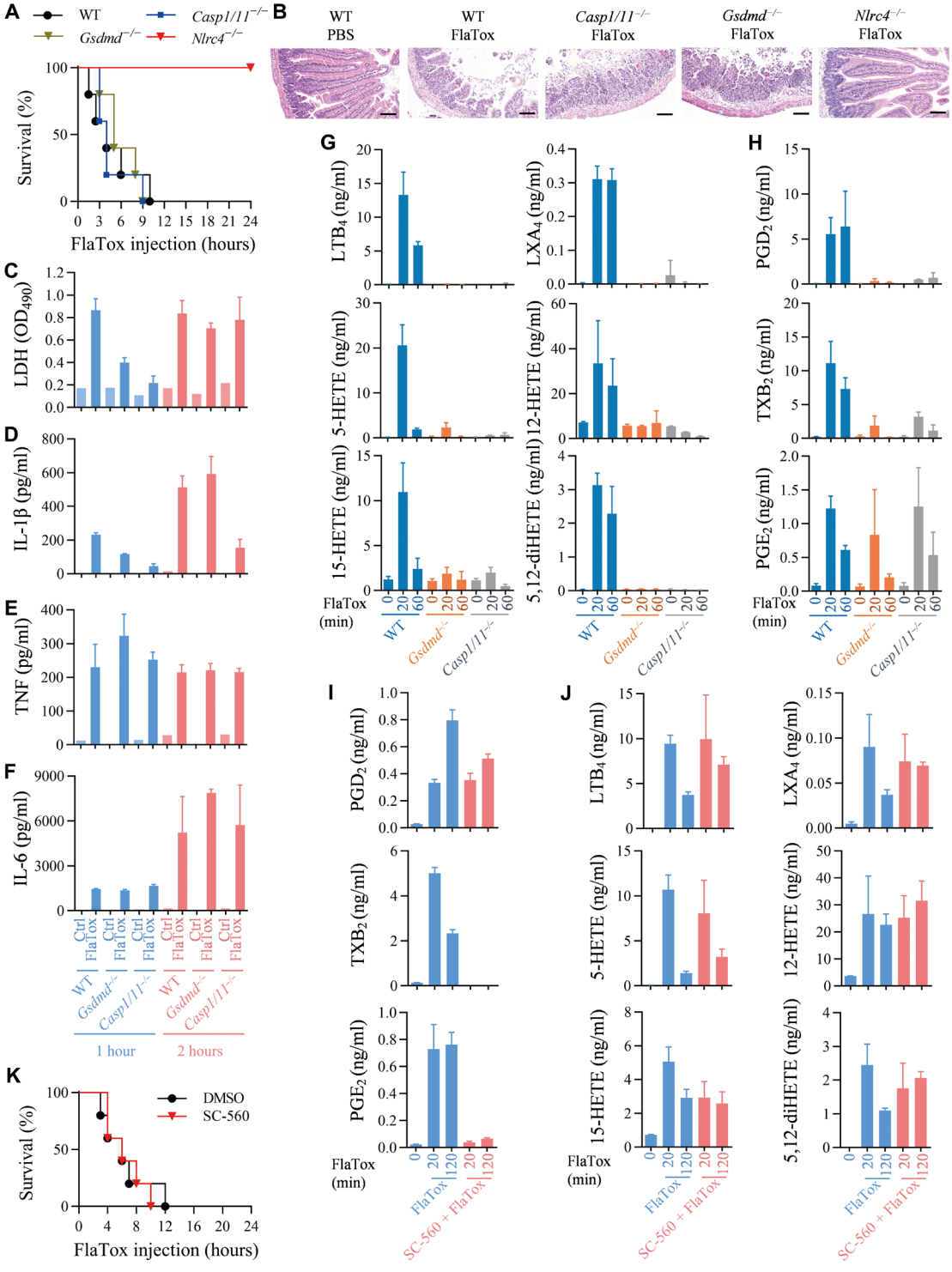

Fig. 1. Release of LDH, a cytolysis indicator, but not inflammatory cytokines or lipid mediators into peritoneal lavages is correlated with NLRC4 inflammasome–triggered mouse death. (**A**) Mice of indicated genotypes were intraperitoneally injected with FlaTox [LFn-Fla (4 μg/g body weight) and PA (2 μg/g body weight)] and monitored for survival rate ($n = 5$). (**B**) Hematoxylin and eosin (H&E) staining of small intestinal tissue of mice treated as indicated for 2 hours. Scale bars, 100 μm. (**C** to **F**) Mice of indicated genotypes were intraperitoneally injected with FlaTox. Peritoneal lavages were isolated by using 1 ml of PBS at 1 and 2 hours after FlaTox challenge and then subjected to measurements of LDH (C), IL-1β (D), TNF (E), and IL-6 (F). $n = 1$ for PBS group (Ctrl) and $n = 3$ for FlaTox-treated group. (**G** and **H**) Mice of indicated genotypes were intraperitoneally injected with FlaTox for indicated times, and peritoneal lavages were collected for liquid chromatography tandem mass spectrometry (LC/MS/MS)–based lipidomics ($n = 3$). (**I** to **K**) Mice of indicated genotypes were pretreated intraperitoneally for 30 min with of COX-1 inhibitor (SC-560) (5 μg/g body weight). Mice were intraperitoneally injected with FlaTox for indicated times, and peritoneal lavages were collected for LC/MS/MS-based lipidomics ($n = 3$). Survival rate was monitored (K) ($n = 5$).

when *Casp1* was deleted (*20*, *21*). We showed previously that *Gsdmd* deletion also switched NLRP3 inflammasome–mediated pyroptosis to apoptosis (*7*) and here that *Gsdmd* deletion has the same effect on cell death induced by AIM2 inflammasome (fig. S3, A to C). Caspase-1–GSDMD axis controls pyroptosis, and deletion of either *Casp1* or *Gsdmd* switches NLRP3- and AIM2-mediated pyroptosis to apoptosis.

To determine whether the switch to apoptosis also occurs in the activation of inflammasomes such as NLRC4 where ASC is not required, we used peritoneal macrophages from *Gsdmd*$^{-/-}$ mice. FlaTox induced pyroptosis in vitro in peritoneal macrophages as measured by LDH release, which was blocked by *Gsdmd* gene deletion (Fig. 2A). However, cytolysis still occurred at later times and reached a comparable level to that of WT macrophages at 8 hours (Fig. 2A). To understand what caused the later cytolysis, we used intracellular adenosine triphosphate (ATP) loss as a general indicator of cell death. Deletion of *Gsdmd* only inhibited about 20% of cell death at 4 hours (Fig. 2B), suggesting that cell death in a form other than pyroptosis occurred in *Gsdmd*$^{-/-}$ macrophages, and this type of cell death might be responsible for the later cytolysis. To better define the cell death pathway, we measured activities of different caspases. *Gsdmd* deletion did not affect FlaTox-induced autocleavage of caspase-1 as revealed by Western blotting (Fig. 2C). In contrast, activation of caspase-8 and caspase-3 was detected in FlaTox-treated *Gsdmd*$^{-/-}$ but not WT cells (Fig. 2, D and E), indicating that activation of pathways leads to apoptosis in *Gsdmd*$^{-/-}$ cells. Western blotting analysis also showed the cleavage of caspase -8 and caspase-3 in *Gsdmd*$^{-/-}$ cells (Fig. 2C), supporting our speculation that there is activation of an apoptotic pathway.

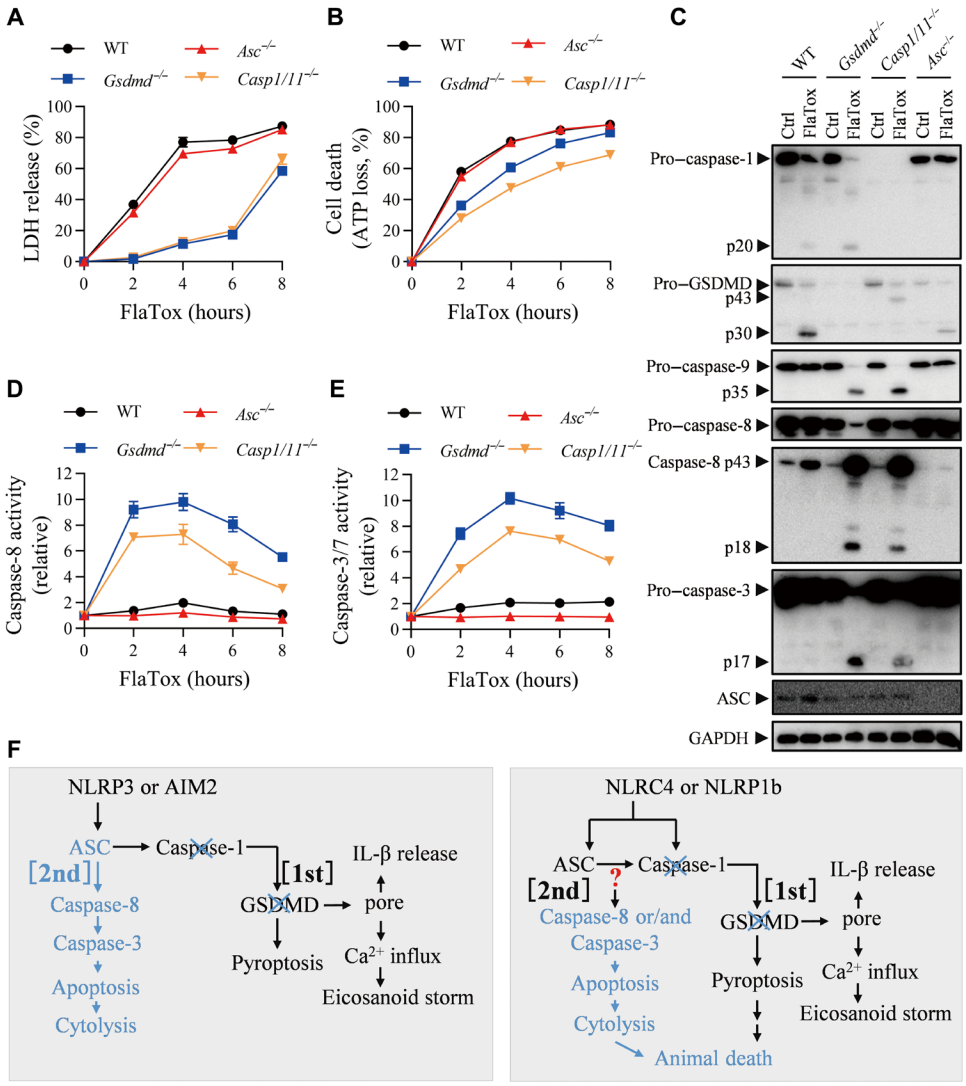

Fig. 2. The effects of genetic deletion of *Gsdmd*, *Caspase-1/11*, or *Asc* on NLRC4 inflammasome–mediated IL-1β secretion, cell death and type of cell death, and mice death. (**A** to **E**) Peritoneal macrophages of indicated genotypes were treated with FlaTox [LFn-Fla (2 μg/ml) and PA (2 μg/ml)] for indicated times. LDH release (A) and ATP loss (B) were measured. Cell lysates combined with medium were subjected to Western blot for indicated proteins (C). Caspase-8 activity (D) and caspase-3/7 activity (E) in cell lysates were measured. Graphs show means ± SE from three independent experiments. (**F**) Model of the death paths. Blue color is used to indicate that this pathway is activated if the other death pathway was blocked. Note that LDH release is an indicator of pyroptosis, ATP loss is an indicator of cell death of any types, and caspase-8 and caspase-3 activations are indicators of apoptosis. GAPDH, glyceraldehyde-3-phosphate dehydrogenase.

As caspase-1 is essential for NLRC4-induced pyroptosis, we used *Casp1/11*$^{-/-}$ peritoneal macrophages to analyze the role of caspase-1 in FlaTox-induced NLRC4 inflammasome activation. Similar to the loss of *Gsdmd*, deletion of *Casp1* effectively blocked FlaTox-induced pyroptosis (Fig. 2A), but we still could detect cell death (Fig. 2B). As expected, we cannot detect caspase-1 in caspase-1–deficient cells (Fig. 2C). Activation of caspase -8 and caspase-3 was observed in caspase-1–deficient cells after FlaTox treatment (Fig. 2, C to E), supporting our contention that when pyroptosis was blocked, cells switched to apoptosis. Collectively, we proposed that since the secondary necrotic lysis of apoptotic cells occurs in vitro, the release of LDH at later time in Fig. 2A should be caused by apoptosis.

ASC is dispensable for NLRC4 inflammasome activation, but its presence can enhance NLRC4 inflammasome–mediated pyroptosis and cytokine production (*14*, *29*, *30*). We used peritoneal macrophages from *Asc* KO mice to address the role of ASC in FlaTox-induced pyroptosis. Deletion of *Asc* had almost no effect on FlaTox-induced pyroptosis (LDH release) (Fig. 2A) and apoptosis (Fig. 2, B to E). Autocleavage of caspase-1 was not detected in FlaTox-treated *Asc* KO cells, but the cleavage of GSDMD was detected (Fig. 2C). These data are consistent with published findings that pro–caspase-1 in inflammasome cleaves GSDMD (*7*). Unlike the deletion of *Gsdmd* or *Casp1*, caspase-8 and caspase-3 activation cannot be detected in *Asc*-deficient cells (Fig. 2, C to E). These data clearly show that deletion of *Asc* did not alter the mechanisms of cell death in FlaTox-treated macrophages.

We then explored whether the deletion of *Gsdmd* or *Casp1* switches NLRP1b inflammasome–induced pyroptosis to apoptosis. RAW264.7 cell is a murine macrophage cell line in which NLRP1b inflammasome activation can be triggered by lethal toxin (LT; lethal factor plus PA) (*31*–*35*). Note that RAW264.7 cells lack ASC; RAW-asc is a RAW264.7-derived cell line containing ectopically expressed ASC (*7*). We confirmed that LT-induced pyroptosis in RAW264.7 and RAW-asc cells can be completely abolished by *Nlrp1b* deletion (fig. S4, A to C). Similar to what we observed in NLRC4 inflammasome activation, *Casp1* or *Gsdmd* deletion blocked pyroptosis, but cells died via apoptosis instead (fig. S5, A to E). Similar data were obtained when J774, another murine cell line, was used (fig. S5, F to J).

The data aforementioned support the idea that LDH release can be resulted directly from pyroptosis and indirectly from apoptosis. To explain the underlying mechanisms on the basis of the above results, we summarized pathway switches from pyroptosis to apoptosis in canonical inflammasome activation and their proposed function in vivo (Fig. 2F). Blockage of caspase-1–GSDMD path [named (first) path] inhibits pyroptosis and allows apoptosis instead. Inhibition of the first path blocks IL-1β/18 release and eicosanoids production. ASC is known to recruit caspase-8 [named (second) death path here] when the first path was impaired during NLRP3 or AIM2 inflammasome activation. On the basis of the data described above, we do not know at this moment which molecule(s) is responsible for caspase-8 activation in FlaTox- or LT-treated *Casp1*- and/or *Gsdmd*-deficient cells. Nonetheless, we can conclude that apoptosis backs up pyroptosis in canonical inflammasomes, regardless of whether ASC is an indispensable or dispensable component of the given inflammasome, and not only pyroptosis but also apoptosis can be downstream of inflammasome activation to elicit cytolysis, which is likely the cause of animal death.

Completely preventing cell death by simultaneously impairing ASC–caspase-8 apoptotic and caspase-1–GSDMD pyroptotic pathways inhibits NLRC4 overactivation–mediated animal death

Although deletion of *Asc* did not affect FlaTox- or LT-induced pyroptosis, we next asked whether ASC is needed for caspase-8 activation and subsequent apoptosis when *Casp1* was deleted. Therefore, we used *Asc*$^{-/-}$*Casp1/11*$^{-/-}$ (triple KO) mice and cells to address this question. Neither FlaTox-induced LDH release nor ATP loss was detected in *Asc*$^{-/-}$*Casp1/11*$^{-/-}$ macrophages (Fig. 3, A and B), indicating a complete block of pyroptosis and apoptosis. Consistently, activation of caspases was also blocked in *Asc*$^{-/-}$*Casp1/11*$^{-/-}$ macrophages (Fig. 3, C to E, and fig. S6A).

Genetic deletion of either *Casp1/11*$^{-/-}$ or *Asc*$^{-/-}$ had almost no effect on FlaTox-induced mouse death (Figs. 1A and 3F). Amazingly, *Asc*$^{-/-}$*Casp1/11*$^{-/-}$ mouse is completely resistant to FlaTox-induced death (Fig. 3, F and G), supporting the idea that cell death is the key determinant in the lethality of animal. Since the function of ASC is to mediate caspase-8 activation when *Casp1* was deleted, we additionally tested whether caspase-1 inhibitor belnacasan plus pan caspase inhibitor emricasan can affect FlaTox-induced mouse death. These inhibitors indeed attenuated FlaTox-induced mouse death (Fig. 3H).

We collected peritoneal lavages from the *Asc*$^{-/-}$*Casp1/11*$^{-/-}$ mice challenged with FlaTox for analyzing caspase activities, LHD release, levels of cytokines, and lipid mediators. Caspase-1, caspase-8, and caspase-3/7 activities (Fig. 3, I to K); LDH release (Fig. 3L); and IL-1β secretion (Fig. 3M) were found to be completely blocked. As it was observed in *Gsdmd*$^{-/-}$ and *Casp1/11*$^{-/-}$ mice, TNF or IL-6 released into peritoneal cavity was not affected in *Asc*$^{-/-}$*Casp1/11*$^{-/-}$ mouse (Fig. 3, N and O). The generation of eicosanoids was almost completely eliminated in *Asc*$^{-/-}$*Casp1/11*$^{-/-}$ mouse except for PGE_2 (Fig. 3, P and Q). Similar to what had been observed in *Nlrc4*$^{-/-}$ mice (fig. S1, K to N), FlaTox-induced increase of blood LDH, IL-1β, TNF, and IL-6 was blocked by deletion of *Asc* and *Casp1/11* (Fig. 3, R to U). As for the increase of circulating TNF and IL-6 in FlaTox-treated mice, its association with LDH release was observed again. To this end, we can conclude that LDH release is downstream of apoptosis, and only LDH release consistently correlates with mouse death.

We used RAW264.7 cells to examine the effect of *Asc* and *Casp1* double KO on LT-induced cell death. Since RAW264.7 cells do not express ASC, RAW-asc cells were included in the experiments. We found that LT did not induce LDH release, ATP loss, activation of caspases in the cells without caspase-1, and ASC expression (fig. S7). Collectively, our data indicate that although ASC is not required for NLRC4 and NLRP1b inflammasome activation, it is required for NLRC4- and NLRP1b-mediated apoptosis in *Casp1*-deficient cells (Fig. 3V). Thus, the (second) death path also functions in canonical inflammasomes, including those that ASC participates in but not required for their activation. As for the FlaTox-induced mice death per se, cell death dictates animal death.

Salmonella Typhimurium is a type of flagellin-producing bacteria whose infection can cause host death (*36*). The animal death by *Salmonella* infection is mainly based on the bacterial dissemination in the host, and inflammasome-mediated immune responses are known to be important in limiting the bacterial burden in vivo as genetic deletion of *Nlrc4*, *Asc*, or *Casp1* leads to increased susceptibility to *Salmonella* infection (*37*–*39*). However, when the in vivo

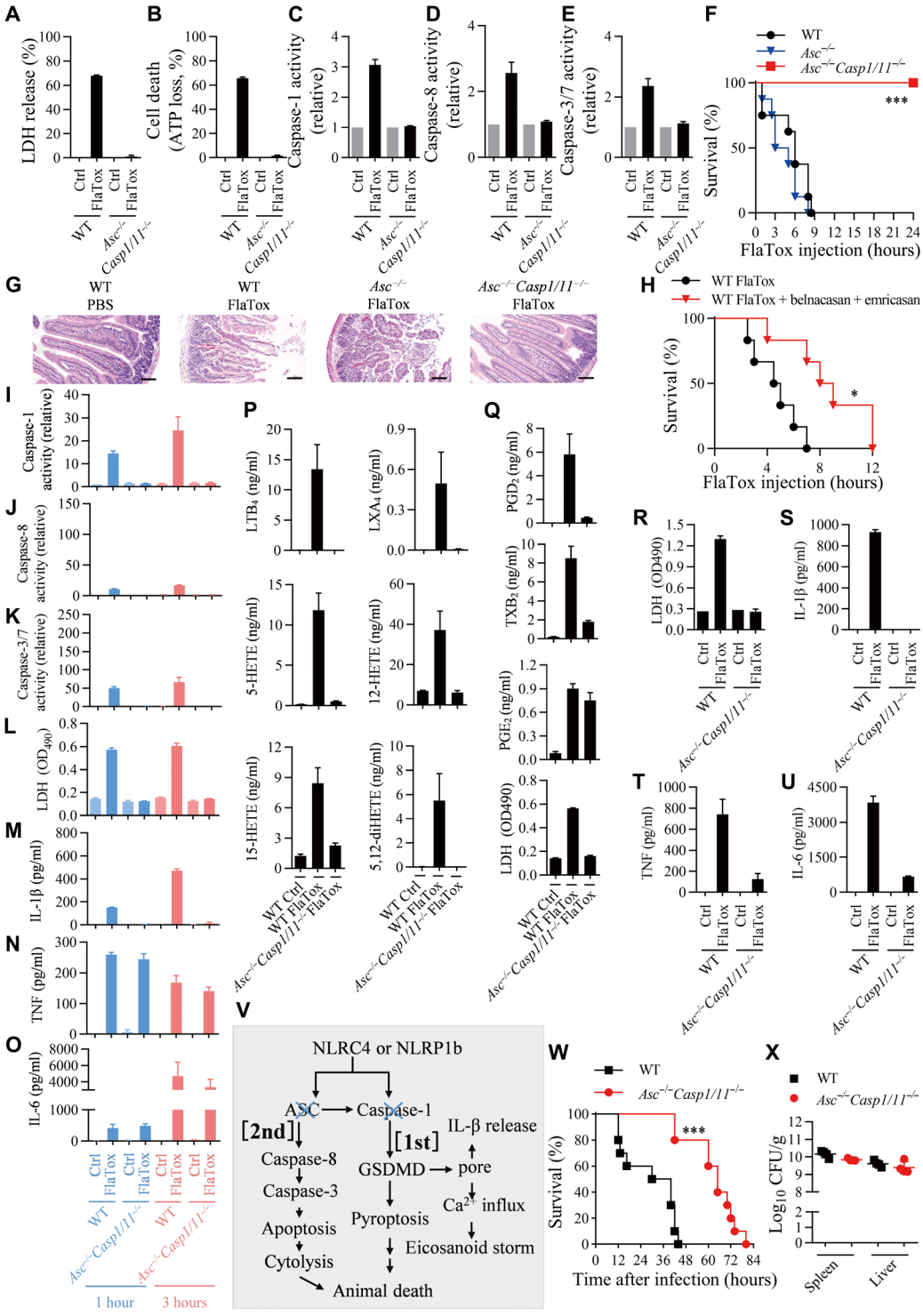

Fig. 3. KO of *Casp1/11* and *Asc* completely blocks FlaTox-induced cell death and mouse death. (**A** to **E**) Peritoneal macrophages were treated with FlaTox for 4 hours. LDH release (A), ATP loss (B), caspase-1 (C), caspase-8 (D), and caspase-3/7 activities (E) were measured ($n = 3$). (**F**) FlaTox-treated mice were monitored for survival ($n = 8$). (**G**) H&E staining of small intestinal tissue of mice treated for 3 hours. Scale bars, 100 μm. (**H**) WT mice were intraperitoneally injected with FlaTox, or FlaTox + belnacasan (100 mg/kg body weight) + emricasan (20 mg/kg body weight) and were monitored for survival ($n = 6$). (**I** to **U**) Peritoneal lavages from FlaTox-treated mice were isolated at 1 hour and 3 hours for caspase-1 (I), caspase-8 (J), caspase-3/7 (K), LDH (L), IL-1β (M), TNF (N), and IL-6 (O) ($n = 3$). Peritoneal lavages at 20 min were collected for LC/MS/MS-based lipidomics (P and Q) ($n = 3$). Serum was used for LDH (R), IL-1β (S), TNF (T), and IL-6 (U). $n = 1$ for PBS group and $n = 3$ for FlaTox-treated mice. (**V**) Model of death paths. (**W** and **X**) Mice were infected with *Salmonella* SL7207 and monitored for survival ($n = 10$). The bacterial loads in spleen and liver were analyzed at the time of mice death ($n = 4$). Graphs show means ± SE. OD_{490}, optical density at 490 nm.

propagation of *Salmonella* was limited by using a propagation-defective SL7207 strain (*40*, *41*), the *Asc*$^{-/-}$*Casp1/11*$^{-/-}$ mice were significantly more resistant to *Salmonella* infection–caused host death in comparison with WT mice (Fig. 3, W and X). It appears that *Salmonella* propagation–caused in vivo pathological changes masked the pivotal role of cell death in animal death since the primary difference between WT and SL7207 strain is that WT but not SL7207 *Salmonella* propagates in mice. It seems that host responses to the process of *Salmonella* propagation but not the amount of bacteria loading in above experimental conditions are important for animal death as bacteria amounts in the spleen and liver had no correlation with the sensitivity to animal death (Fig. 3X). Inhibition of bacteria propagation in vivo is a primary therapeutic approach in treating infectious diseases, which could demask the decisive role of cell death in animal death, and inhibition of death pathways could be a clinically relevant cotreatment for lethal infections.

Asc and *Gsdmd* double KO does not prevent mice from NLRC4 inflammasome–induced lethality because a caspase-1–dependent apoptosis pathway (the third path) is activated to arbitrate mouse death

Figure 3F shows that *Asc* and *Casp1* double KO completely blocked FlaTox-induced mouse death, but unexpectedly, double deletion of *Asc* and *Gsdmd* did not protect the animal from death (Fig. 4A). We obtained peritoneal cells by lavage from FlaTox-challenged mice and analyzed their caspase activities, cytokines, and LDH release. Caspase-1 activation was impaired in *Asc*$^{-/-}$*Gsdmd*$^{-/-}$ sample at 1 hour but reached WT level at 3 hours (Fig. 4B). Significantly, more caspase-8 and caspase-3/7 activation was observed in *Asc*$^{-/-}$*Gsdmd*$^{-/-}$ lavages (Fig. 4, C and D). LDH release in *Asc*$^{-/-}$*Gsdmd*$^{-/-}$ lavages was not detected at early time (1 hour) but reached to a comparable level of WT lavages at 3 hours (Fig. 4E). Western blotting data revealed patterns of caspase cleavage that mirror results from enzymatic assays (fig. S6A). Similar to the deletion of *Gsdmd* (Fig. 1D), double deletion of *Asc* and *Gsdmd* did not affect the secretion of IL-1β into peritoneal cavity in FlaTox-treated mice (Fig. 4F). The production of TNF and IL-6 is not related to inflammasome activation and was not affected by double deletion of *Asc* and *Gsdmd* (Fig. 4, G and H). In addition, double deletion of *Asc* and *Gsdmd* did not affect the tissue damage (fig. S6B). The activation of apoptotic caspases indicates the occurrence of apoptosis, and the later LDH release is most likely caused by secondary necrosis of apoptosis.

We then analyzed the death of macrophages from those KO mice in vitro (Fig. 4, I to M). The cells with double deletion of *Asc* and *Gsdmd* behaved more like *Gsdmd*$^{-/-}$ other than *Asc* and *Casp1* double KO in terms of protecting cells from death caused by NLRC4 or NLRP1b inflammasome (Figs. 1 and 4, I to M, and fig. S6A). FlaTox-induced LDH release was blocked in *Asc*$^{-/-}$*Gsdmd*$^{-/-}$ peritoneal macrophages until 4 hours, but ATP loss was only partially inhibited at this time point (Fig. 4, I and J). With the evidence of apoptotic caspase activation (Fig. 4, L and M, and fig. S6A), we believe that the cell death mode was apoptosis. Because *Asc*$^{-/-}$*Casp1/11*$^{-/-}$ cells were completely protected from NLRC4- or NLRP1b-mediated death (Fig. 3, A to E, and fig. S5), caspase-1 activation (Fig. 4K) observed in *Asc*$^{-/-}$*Gsdmd*$^{-/-}$ cells must be required for their apoptotic death.

The effect of *Asc* and *Gsdmd* double KO on LT-induced cell death was evaluated using RAW264.7 cells, and the data show that cells with no *Asc* and *Gsdmd* undergo apoptosis upon LT stimulation (fig. S7). It appears that caspase-1 is capable of triggering apoptosis when both *Asc* and *Gsdmd* were deleted, and we called this caspase-1–dependent apoptosis pathway the (third) death path (Fig. 4N).

The third path is caspase-1–activated intrinsic apoptotic pathway

As RAW264.7 cell is not sensitive to FlaTox, we used LT stimulation of RAW264.7 cells to study the caspase-1–dependent apoptosis. We measured LT-induced LDH release and ATP loss in RAW-asc and its *Gsdmd*$^{-/-}$, *Gsdmd*$^{-/-}$*Casp8*$^{-/-}$, and *Gsdmd*$^{-/-}$*Casp8*$^{-/-}$*Casp1*$^{-/-}$ cell lines at 4 hours after LT treatment. Deletion of *Gsdmd* and *Casp8* inhibited LDH release (Fig. 5A), but significant ATP loss occurred in *Gsdmd*$^{-/-}$*Casp8*$^{-/-}$ cells (Fig. 5B), suggesting that it was caspase-1 that triggered cell death in the absence of caspase-8 and GSDMD (third death path). *Gsdmd*$^{-/-}$*Casp8*$^{-/-}$*Casp1*$^{-/-}$ cells are fully resistant to LT-induced cell death (Fig. 5, A to F). Caspase-3 activation should be downstream of caspase-1 since the increase of caspase-3 activity in LT-treated *Gsdmd*$^{-/-}$*Casp8*$^{-/-}$ cells was observed by enzymatic assay and Western blotting (Fig. 5, C to F). Thus, the third death pathway should be caspase-1 → caspase-3 → apoptosis. Consistently, RAW-asc *Casp8*$^{-/-}$*Casp1*$^{-/-}$ cells were fully resistant to LT-induced cell death (fig. S8).

It is known that oligomerization of ASC is required for ASC to function in all subtype inflammasomes (*1*). Since both caspase-1 and caspase-8 can interact with ASC, we analyzed ASC oligomerization in *Gsdmd*$^{-/-}$, *Gsdmd*$^{-/-}$*Casp8*$^{-/-}$, and *Gsdmd*$^{-/-}$*Casp8*$^{-/-}$*Casp1*$^{-/-}$ RAW-asc cell lines. Cross-link and immunostaining of ASC in these different cells were performed before and after LT treatment. Results showed that LT-induced oligomerization and speck formation of ASC were not influenced by the single, double and triple deletions (Fig. 5, G and H). These data excluded the possibility that there was reverse signaling to affect ASC oligomerization when GSDMD, caspase-8, and caspase-1 were impaired.

Caspase-1 (IL-lβ–converting enzyme) was reported to induce apoptosis in fibroblasts (*42*), and the cleave BH3-interacting domain death agonist (Bid) at D59 by caspase-1 could be the underlying mechanism as the cleaved Bid activates intrinsic apoptosis pathway (*43*–*46*). To determine whether intrinsic apoptosis plays a role in the third pathway, we deleted *Apaf1* in *Gsdmd/Casp8* double KO RAW-asc cells and found that it inhibited LT-induced ATP loss (apoptosis) (Fig. 6, A to E) but did not affect caspase-1 activation in RAW-asc *Gsdmd*$^{-/-}$*Casp8*$^{-/-}$ cells (Fig. 6C). Enzymatic assay and Western blotting confirmed abrogation of LT-induced caspase-9 and caspase-3 activation by this additional *Apaf1* deletion (Fig. 6, C to E). Consistently, deletion of *Casp9* in RAW-asc *Gsdmd*$^{-/-}$*Casp8*$^{-/-}$ cells also inhibited LT-mediated apoptosis (Fig. 6, A to E). We also measured IL-1β release by lipopolysaccharide (LPS)–primed RAW-asc cells with various gene deletions and found that LT-induced IL-1β release was partially blocked in *Gsdmd*$^{-/-}$ cells and completely eliminated in *Gsdmd*$^{-/-}$*Casp8*$^{-/-}$, *Gsdmd*$^{-/-}$*Casp8*$^{-/-}$*Apaf1*$^{-/-}$, and *Gsdmd*$^{-/-}$*Casp8*$^{-/-}$*Casp9*$^{-/-}$ cells (Fig. 6F). The caspase-1–dependent activation of caspase-3 and apoptosis in *Asc* and *Gsdmd* double-deficient (RAW264.7 *Gsdmd*$^{-/-}$) cells were blocked by genetic deletion of *Casp9* (fig. S9). The modest activation of caspase-8 was also observed in *Asc* and *Gsdmd* double-deficient cells, which was abrogated by genetic deletion of *Casp9* (fig. S9). This caspase-9–dependent activation of caspase-8 may be attributed to a caspase-3 feedback signal reported previously (*47*). Thus, caspase-1–induced apoptosis is primarily mediated by the intrinsic apoptosis pathway (apaf1 → caspase-9 → caspase-3) (Fig. 6G).

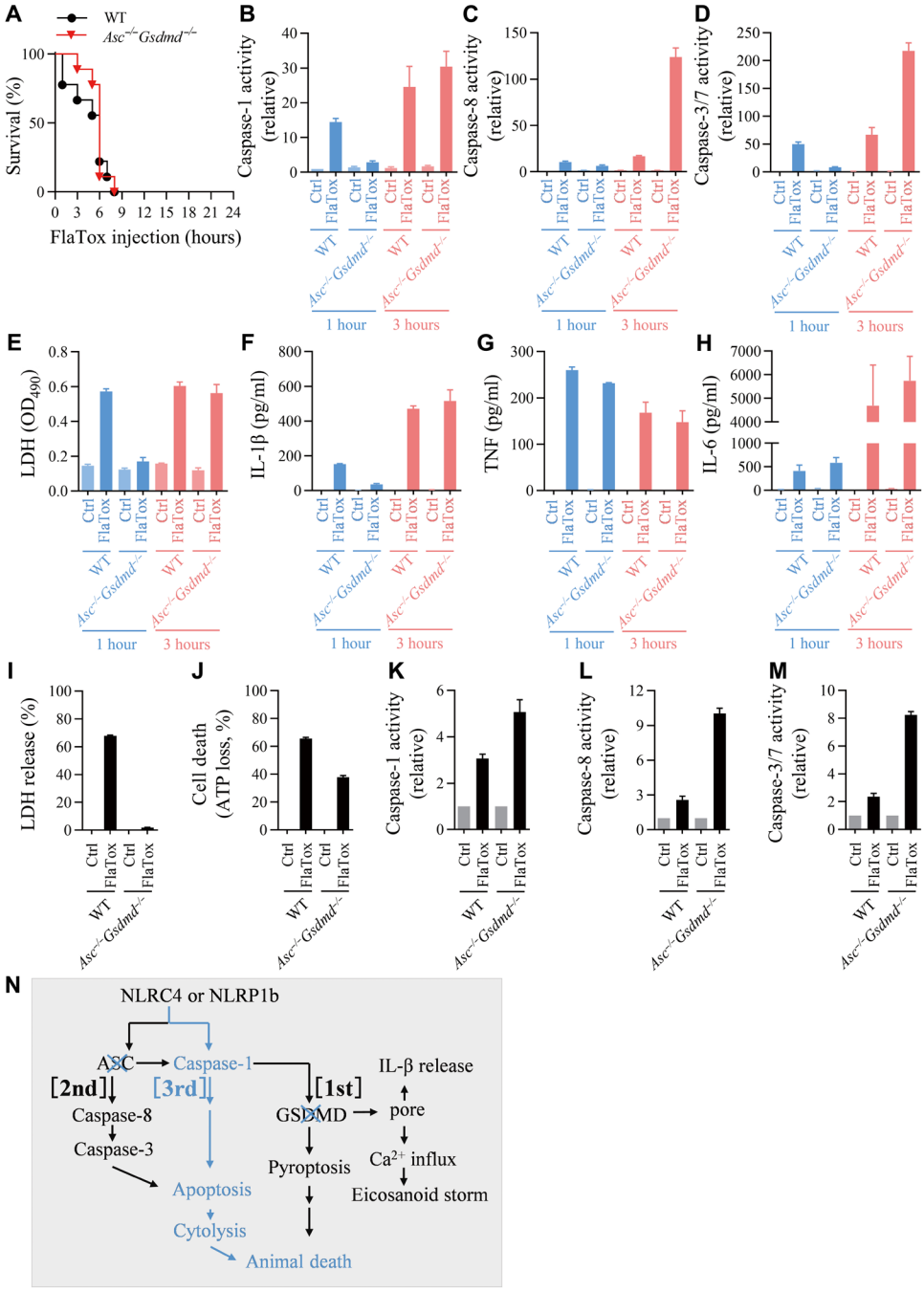

Fig. 4. Double KO of *Gsdmd* and *Asc* cannot block FlaTox-induced cell death and mouse death. (**A** to **H**) Mice of indicated genotypes were intraperitoneally injected with FlaTox (4 μg/g LFn-Fla body weight and 2 μg/g PA body weight) and monitored for survival (A) at indicated times ($n = 9$). Peritoneal lavages were isolated by using 1 ml PBS at 1 and 3 hours after FlaTox challenge and then subjected to measurements of caspase-1 activity (B), caspase-8 activity (C), caspase-3/7 activity (D), LDH (E), IL-1β (F), TNF (G), and IL-6 (H) ($n = 3$). (**I** to **M**) Peritoneal macrophages from mice of indicated genotypes were treated with FlaTox (2 μg/ml LFn-Fla and 2 μg/ml PA) for 4 hours. The LDH release (I) and ATP loss (J) were measured. The caspase-1 activity (K), caspase-8 activity (L), and caspase-3/7 activity (M) were measured. Graphs show means ± SE from three independent experiments. (**N**) Model of the death paths.

The third death path can also be induced by the activation of NLRP3 or AIM2 inflammasome if *Gsdmd* and *Casp8* were deleted

Next, we sought to determine whether the third death path can be activated by NLRP3 and AIM2 inflammasomes. NLRP3- and AIM2-dependent inflammasome activation was induced by LPS plus nigericin or LPS plus Poly (dA:dT), respectively, in RAW-asc and its *Gsdmd*$^{-/-}$, *Gsdmd*$^{-/-}$*Casp8*$^{-/-}$, and *Gsdmd*$^{-/-}$*Casp8*$^{-/-}$*Casp1*$^{-/-}$ cells. Microscopy revealed that NLRP3 or AIM2 inflammasome activation leads to pyroptosis in RAW-asc cells, apoptosis in *Gsdmd*$^{-/-}$ and

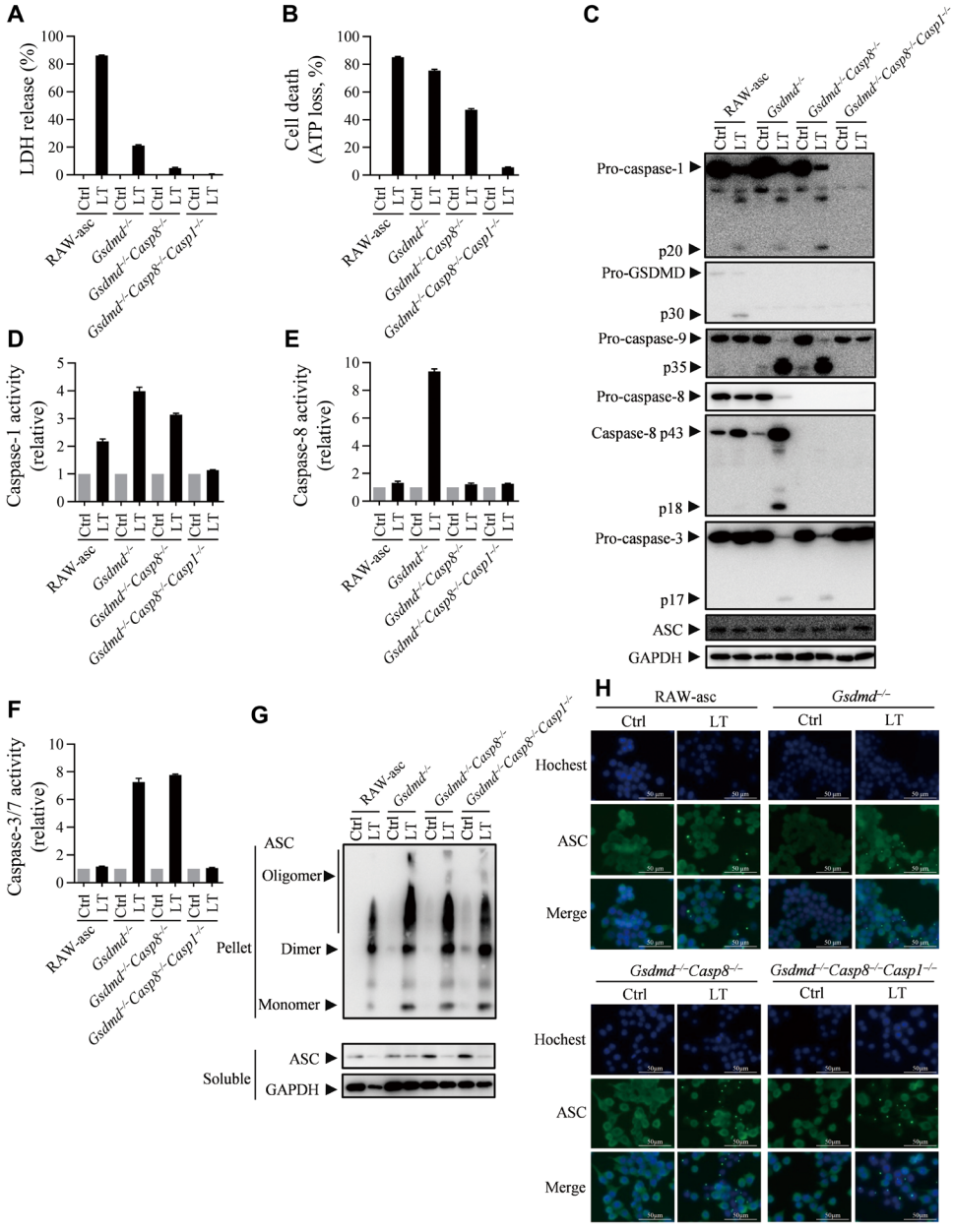

Fig. 5. Caspase-1 is responsible for NLRP1b inflammasome–mediated apoptosis in *Gsdmd* and *Casp8* double deleted cells. (**A** to **F**) RAW-asc cells of indicated genotypes were treated with LT (2 μg/ml LF and 2 μg/ml PA) for 4 hours. LDH release (A) and ATP loss (B) were measured. Cell lysates combined with medium were subjected to Western blot for indicated proteins (C). Caspase-1 activity (D), caspase-8 activity (E), and caspase-3/7 activity (F) were measured. (**G** and **H**) RAW-asc cells of indicated genotypes were treated with LT for 90 min. ASC oligomerization was analyzed by cross-linking and Western blotting (G), and speck formation was viewed under confocal microscope (H). Graphs show means ± SE from three independent experiments.

Gsdmd$^{-/-}$*Casp8*$^{-/-}$ cells, and no death of *Gsdmd*$^{-/-}$*Casp8*$^{-/-}$*Casp1*$^{-/-}$ cells (Fig. 7A). We also analyzed oligomerization of ASC in LPS plus nigericin or LPS plus Poly (dA:dT)–treated RAW-asc cells and found that ASC oligomerized normally in *Gsdmd*$^{-/-}$, *Gsdmd*$^{-/-}$*Casp8*$^{-/-}$, and *Gsdmd*$^{-/-}$*Casp8*$^{-/-}$*Casp1*$^{-/-}$ cells (Fig. 7B). The IL-1β induction by Poly (dA:dT) in LPS-primed RAW-asc cells was partially blocked in *Gsdmd*$^{-/-}$ cells and completely eliminated in *Gsdmd*$^{-/-}$*Casp8*$^{-/-}$ and *Gsdmd*$^{-/-}$*Casp8*$^{-/-}$*Casp1*$^{-/-}$ cells (Fig. 7C). As anticipated, caspase-1 activation was detected in all cells except *Gsdmd*$^{-/-}$*Casp8*$^{-/-}$*Casp1*$^{-/-}$ cells (Fig. 7D), and caspase-8 activation was only detected in *Gsdmd*$^{-/-}$ but not WT (RAW-asc), *Gsdmd*$^{-/-}$*Casp8*$^{-/-}$, and *Gsdmd*$^{-/-}$*Casp8*$^{-/-}$*Casp1*$^{-/-}$ cells (Fig. 7E). Caspase-3/7 activity was detected not only in *Gsdmd*$^{-/-}$ cells but also in *Gsdmd*$^{-/-}$*Casp8*$^{-/-}$ cells (Fig. 7F), demonstrating that the third death path (caspase-1 → caspase-3) was activated by NLRP3 and AIM2 inflammasomes when both GSDMD-mediated pyroptosis and caspase-8–mediated apoptosis were inhibited (Fig. 7G). These results indicate that the third death path appears to be universally used by canonical inflammasomes. We also have data that THP1 *CASP1*$^{-/-}$*CASP8*$^{-/-}$ cells are fully resistant to NLRP3 and AIM2 inflammasome–mediated

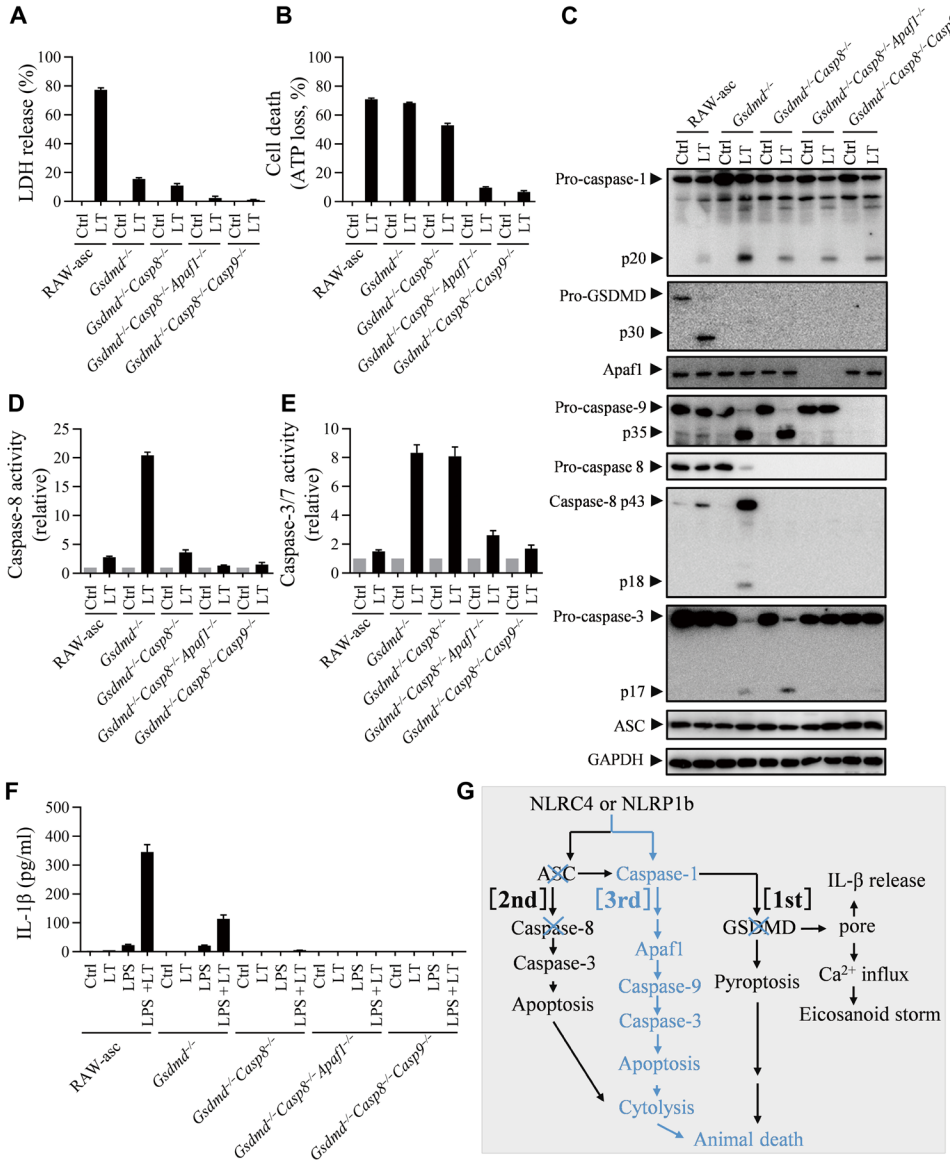

Fig. 6. Caspase-1–initiated apoptosis during NLRP1b inflammasome activation is mediated by Apaf1–caspase-9 intrinsic apoptotic pathway. (**A** to **E**) RAW-asc cells of indicated genotypes were treated with LT [LF (2 μg/ml) and PA (2 μg/ml)] for 4 hours. The LDH release (A) and ATP loss (B) were measured. Cell lysates combined with medium were subjected to Western blot for indicated proteins (C). The caspase-8 activity (D) and caspase-3/7 activity (E) were measured. (**F**) RAW-asc cells of indicated genotypes were pretreated with or without LPS (500 ng/ml) for 4 hours and then stimulated with LT for 2 hours. The IL-1β in supernatant was measured by enzyme-linked immunosorbent assay (ELISA). (**G**) Model of the death paths. Graphs show means ± SE from three independent experiments.

cell death (fig. S10), indicating that our conclusion could extend to human cells. Thus, targeting both ASC and caspase-1 or both caspase-1 and caspase-8 is a potential therapeutic way to block cell death driven by canonical inflammasome activation, which may help to prevent the lethality caused by inflammasome overactivation.

DISCUSSION

Inflammasome-mediated cell death on one hand contributes to the activation of immune system to control infected pathogens (*14*–*18*). On the other hand, cell death by itself subsidizes the pathological changes in infected animals (*17*). The data presented in this report demonstrate that cell death plays a decisive role in the death of mice caused by NLRC4 inflammasome in an infection-free system. In the case of live bacteria, such as *S.* Typhimurium infection, NLRC4-triggered cell death contributes to host death, but the outcome should be determined by multiple factors. Blocking the cell death pathways downstream of NLRC4 attenuated mice death caused by growth-defective *Salmonella* infection (Fig. 3W), but this inhibition was not observed when WT *Salmonella* was used, suggesting that the lethal effect of bacteria propagation is before that of cell death (*37*–*39*). Therefore, if propagation of infected pathogens can be blocked by pharmacological approaches, blocking inflammasome overactivation–caused cell death shall be important for preventing the host from death.

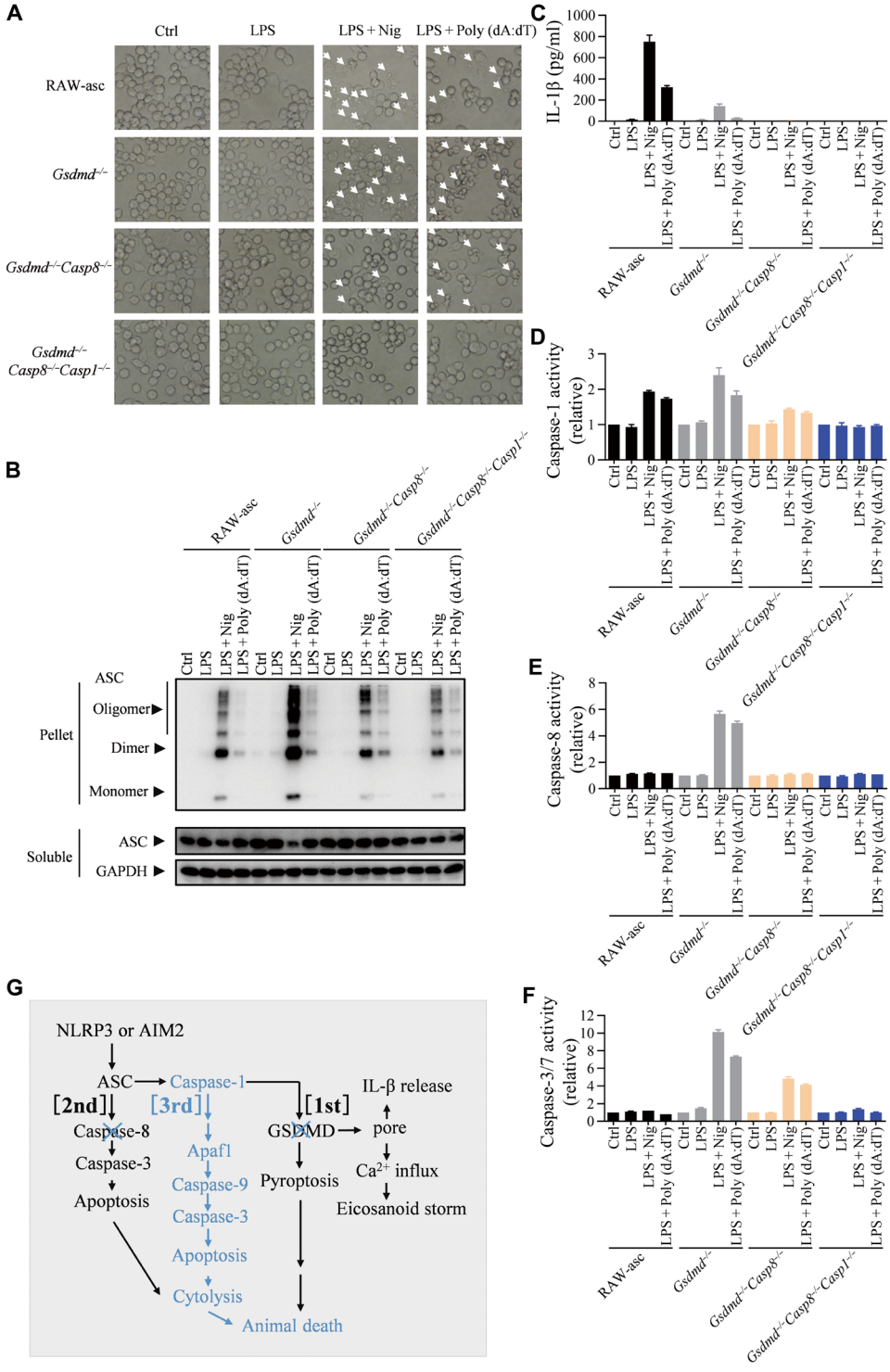

Fig. 7. The third death path also applies to NLRP3 and AIM2 inflammasomes. (**A** to **E**) RAW-asc cells of indicated genotypes were treated with LPS (1 μg/ml) and then stimulated with nigericin (10 μM) or Poly (dA:dT) (2 μg/ml). Arrows indicate pyroptotic or apoptotic cells under microscopy (A). ASC oligomerization was measured at 90 min (B). The IL-1β in supernatant was measured by ELISA (C). Caspase-1 activity (D), caspase-8 activity (E), and caspase-3/7 activity (**F**) were measured. (**G**) Model of the death paths. Graphs show means ± SE from three independent experiments.

A previous study showed that deletion of *Casp1* and *Casp8* (*Casp1*$^{-/-}$*Casp8*$^{-/-}$*Rip3*$^{-/-}$ mice) reduced ability of mice in controlling the propagation of orally infected *S.* Typhimurium (*17*). A recent study further showed that simultaneous genetic deletion of *Casp1*, *Casp11*, *Casp12*, *Casp8*, and *Rip3* ensured the blockade of *Salmonella*-induced cell death and sensitized mice to the infection with a growth-attenuated *Salmonella* Δ*AroA* strain BRD509 (*15*). WT mice were capable of controlling the propagation of intravenously

injected BRD509 [200 colony-forming units (CFU)] within a certain level and eventually clearing the bacteria after 12 weeks, whereas the injected BRD509 in *Casp1*$^{-/-}$*Casp11*$^{-/-}$*Casp12*$^{-/-}$*Casp8*$^{-/-}$*Rip3*$^{-/-}$ mice continued propagating, and the infected mice had to be euthanized in 4 to 5 weeks after infection because of heavy in-organ bacterial burden (*15*). It appears that similar to virus infections, cell death is a mechanism to eliminate intracellular bacteria such as *Salmonella*. In agreement with this notion, animal death caused by high-dose nonpropagative SL7207 was significantly attenuated by blocking NLRC4-mediated cell death (Fig. 3W). Thus, cell death should have dual roles in host defense against intracellular bacteria, and the pro-death role would be predominant if bacteria propagation has been eliminated by other means.

Global induction of the production of inflammatory cytokines, the so-called cytokine storm, is believed to be the major trigger of infection/inflammation-caused animal death. The levels of FlaTox-induced cytokines such as IL-1β, TNF, and IL-6 in mice are comparable to those induced by *S.* Typhimurium infection, indicating the induction of cytokine storm by NLRC4 activation directly or indirectly. However, in line with a published study (*13*), we confirmed that there is no correlation between the levels of IL-1β, TNF, or IL-6 and death in FlaTox-treated mice (Figs. 1 and 3). The increase of circulating TNF and IL-6, an NLRC4-independent response to flagellin, was associated with LDH release (cytolysis) (fig. S1, K to N and S to V, and Fig. 3, R to U). The factors that caused the increase of circulating (blood) TNF and IL-6 in FlaTox-treated cells are very likely to be the damage-associated molecular patterns released from dead cells. We also did not find a correlation between animal death and eicosanoids production. We showed here that eicosanoids production is dependent on pyroptosis (Fig. 1, G and H), which is not unexpected as it was previously proposed that eicosanoid biosynthesis is stimulated by Ca^{2+} influx via FlaTox-induced plasma membrane pore (*13*), which should be GSDMD pore based on current knowledge (*7*–*9*). We proposed that either "cytokine or eicosanoid storm" is not essential for FlaTox-induced animal death, or the animal death is resulted from the compound effect of a large number of different cytokines/lipids, and the commonly used measurement of cytokines cannot evaluate the effect of cytokine storm.

Our data demonstrated that irreversible cell death induced by NLRC4 overactivation definitely can play a decisive role in animal death, which is consistent with a published study by Rauch *et al.* (*17*) showing that deletion of *Casp1* and *Casp8*, which should block all three death pathways described in this study (Fig. 7G), inhibited FlaTox-induced body temperature drop (an indicator of animal viability). Rauch *et al.* (*17*) also showed that *Asc*$^{-/-}$*Casp1/11*$^{-/-}$ and *Rip3*$^{-/-}$*Casp1*$^{-/-}$*Casp8*$^{-/-}$ mice were fully protected from FlaTox-induced pathological changes, including hypothermia, hematocrit increase, diarrhea, intestinal epithelial cell expulsion, PGE_2, and body temperature drop. Our data that FlaTox-induced animal death was prevented by gene deletion of *Asc* and *Casp1/11* are in line with their finding.

Cell death in vivo could be a result of cytokine storm, which, in turn, can induce cytokine production. In the situation of FlaTox-induced sterile NLRC4 activation, cell death is a direct consequence of FlaTox treatment. Pyroptosis is important for the production of some cytokines such as IL-1β and IL-18 and inflammatory lipids, and they could induce other cytokines such as TNF, but those cytokines and lipids are not essential for FlaTox-induced animal death. Bacterial infection, such as *S.* Typhimurium infection, is a much more complicated situation in comparison with the NLRC4 activation by FalTox, and pathway switches such as pyroptosis to caspase-8–dependent apoptosis in *Salmonella*-treated macrophages occur (*15*). The cytokine to cell death and cell death to cytokine circles could function in bacterial infections.

Previous studies have revealed switches among or compensation of different cell death pathways when one of them was absent or impaired (*7*, *8*, *15*, *20*–*22*, *48*, *49*). In this report, we revealed the order of complementation of three distinct cell death pathways in inflammasome-mediated cell death process. It seems that cell death is destined to take place after inflammasome has been fully activated. The inevitable cell death does not necessarily promote IL-1β secretion as there was cell death in FlaTox-treated *Casp1/11*$^{-/-}$ mice but not much IL-1β in peritoneal lavages (Fig. 1, C and D). IL-1β secretion is definitely not a must to reach destination by the inherent complementary cell death pathways. The preferential adoption of these cell death pathways in a specific order could be programmed for animal death since only the mutant mice in which cell death was blocked survived from FlaTox treatment (Figs. 1, A and F, and 4A. Cell death types are not important for outcomes at animal level.

It was reported that GSDMD can be inactivated by caspase-3/-7 when apoptosis occurred (*50*). This is the case in *Casp1*$^{-/-}$ cells when apoptosis was induced by NLRC4, NLRP1b, NLRP3, or AIM2 inflammasome. Cleavage of GSDMD by caspase-8 was also reported to mediate pyroptosis when transforming growth factor β–activated kinase 1 was inhibited (*51*), although we did not detect GSDMD cleavage by caspase-8 in our experimental settings. The cleavage of GSDMD by apoptotic caspases suggests possible inhibition of pyroptosis by apoptosis.

We detected activation of caspase-8 and caspase-9 when the third pathway was activated, and caspase-9 but not caspase-8 is required for the third pathway (Fig. 6). Caspase-8 activation should be an associated event of caspase-9 activation and could be additive but not essential for the third path of inflammasome-induced cell death. Activation of caspase-8 by caspase-9–activated caspase-3 was reported (*47*), and here, it is likely the same case. A recent report showed that forced activation of caspase-1 in cells without GSDMD–induced apoptosis through the Bid → caspase-9 → caspase-3 axis (*46*), supporting the idea that caspase-1 can activate intrinsic apoptotic pathway when pyroptotic pathway is impaired. In addition, cleavage of Bid by caspase-8 can mediate the intrinsic apoptosis pathway (*44*). In the current study, we indeed observed caspase-9 activation in *Casp1*-deficient conditions when NLRC4, NLRP3, AIM2, and NLRP1b inflammasomes were activated (Fig. 2C, and figs. S3C and S5, C and H).

Since FlaTox-induced mouse death is the only model available for lethality solely mediated by inflammasomes, we were unable to evaluate whether hyperactivation of the inflammasomes other than NLRC4 is lethal. Because of similarity among the subtype inflammasomes, we would predict that the conclusion of this study can be applicable to other inflammasomes. However, we shall note that injection of FlaTox in mice is an artificial approach, and unfortunately, there is no model available that can recapitulate NLRC4 activation in a more physiologically relevant setting. Efforts should be given to find relevant stimulus and animal model that can better mimic NLRC4-dependent pathological changes reported in human patients. Nonetheless, the preexistence of three death paths suggests a firm commitment to cell death after inflammasome hyperactivation, which is not important for inflammasome-mediated cytokine

secretion but destined to inflammasome-caused animal death. Cell death, regardless of its type, plays a decisive role in animal death caused by NLRC4 inflammasome hyperactivation. The decisive role of cell death might be applicable to other inflammation-related lethality, such as septic shock. Cell death is a marker of the immunosuppression stage of sepsis, and this phase links to the lethality of septic individuals (*52*, *53*). It is highly possible that inhibition of cell death is an effective cotreatment of lethal infectious diseases when the propagation of infected pathogen can be eliminated by other therapeutic approaches.

MATERIALS AND METHODS

Study design

The objective of this study was to investigate the relation between canonical inflammasome–mediated cell death and host death. We deleted various canonical inflammasome–related genes individually or in combination in cells and mice and analyzed their effects on cell and mouse death as well as death pathways triggered by different canonical inflammasomes. The stimulation and replicates of each experiment are presented in the figure legends.

Mice

All mice used were housed in a specific pathogen-free environment. WT C57BL/6J mice were originally obtained from the Jackson Laboratory. *Casp1/11*$^{-/-}$ and *Gsdmd*$^{-/-}$ mice were used as previously described (*7*). *Asc*$^{-/-}$, *Nlrc4*$^{-/-}$, and *Gsdme*$^{-/-}$ mice were generated by co-microinjection of in vitro translated Cas9 mRNA and guide RNA (gRNA) into the C57BL/6J zygotes. The targeting sequence in the gRNA vector was 5′-CAGACGAGCCCTTATTCAA-3′ for mouse *Nlrc4*, 5′-TATGGGCGCATCCCACGCG-3′ for mouse *Asc*, and 5′-TTCGCCTTTCTGGACATGC-3′ for mouse *Gsdme*. All KO alleles have been crossed onto the C57BL/6J background. Male mice between 8 and 12 weeks of age were used for the animal experiments in the current study. All animal experiments were conducted following the guidelines for housing and care of laboratory animals and performed in accordance with regulations approved by the Animal Care and Use Committee at Xiamen University.

For intraperitoneal injection of FlaTox into mice, toxin doses were PA (2 μg/g body weight) combined with LFn-Fla or LFn-Fla 3A (4 μg/g) and diluted in 250 μl of phosphate-buffered saline (PBS). The survival rate of the animals was checked every few hours.

Generation of KO cell lines using CRISPR-Cas9 technique

The targeting sequence in the gRNA vector was 5′-TCTCTAAAAAGGGCCCC-3′ for mouse *caspase-1*, 5′-TGCAACAGCTTCGGAGTCG-3′ for mouse *Gsdmd*, 5′-TATGGGCGCATCCCACGCG-3′ for mouse *Asc*, 5′- GTCTAGGAAGTTGACCAGC-3′ for mouse *caspase-8*, 5′-GGATGAAGAGCAGCTTCTCA-3′ for mouse *Nlrp1b*, 5′- ATGGATCACATGATCAGTAA-3′ for mouse *Apaf1*, 5′-CTGGCTTCACTCTTGCAAAG-3′ for mouse *caspase-9*, 5′-ATTGACTCCGTTATTCCGAA-3′ for human *CASP1*, and 5′-CCCTCAAGTTCCTGAGCCT-3′ for human *CASP8*. The plasmids (vector pBOB) harboring the gene gRNA sequences and Cas9 gene were transfected into 293T in the presence of lentivirus helper plasmids, and the supernatants were collected after 48 hours. The viruses were then used to infect J774 cells, RAW264.7 cells, RAW-asc cells, or THP1 cells. KOs were confirmed by immunoblots and further confirmed by sequencing.

LFn fusion protein preparation

pET15b LFn-Fla (Addgene plasmid no. 84871) and pET15b LFn-Fla 3A (Addgene plasmid no. 84872) were gifts from R. Vance. The LFn-Fla and LFn-Fla 3A were expressed and purified as described in previous publications (*13*). The endotoxin was removed with the ToxinEraserTM Endotoxin Removal Kit (L00338, GenScript).

Bacterial strains for infection studies

For in vivo infection, *Salmonella* SL7207 (ΔaroA) was incubated with shaking at 37°C in Luria-Bertani (LB) broth for 16 hours, and then 500 μl of medium with bacteria was added to a new tube with 15 ml of LB broth shaking until an optical density at 600 nm (OD_{600}) reached 1.0. The collected *Salmonella* was diluted in PBS, and 5×10^8 CFU for *Salmonella* SL7207 (ΔaroA) were injected intraperitoneally in a volume of 200 μl. The number of bacteria was examined by homogenizing organs of infected mice in 5 ml of sterilized PBS. The homogenate was diluted and plated onto LB agar plates and incubated at 37°C for 16 hours.

Hematoxylin and eosin staining

Animals were euthanized. Small intestines were collected and fixed immediately in 4% paraformaldehyde for 24 hours. The fixed tissues were embedded in a water-free procedure. Five-micrometer sections were cut and stained with hematoxylin and eosin. Slides were analyzed on the Leica Aperio Versa 200.

Eicosanoid analysis

For peritoneal lavage analysis, mice were injected intraperitoneally with FlaTox. After the indicated time, mice were euthanized and injected intraperitoneally with 1 ml of cold PBS. Peritoneal lavage (600 μl) was collected, and 50 μl of which was immediately transferred to 500 μl of cold methanol for storage at −80°C. Eicosanoids and docosanoids were identified and quantified by AB SCIEX QTRAP-6500 plus. The synthetic standards were purchased from Cayman Chemical.

Cell cultures and stimulation

Peritoneal macrophages were isolated from mice after being injected intraperitoneally with 3% thioglycollate solution for 4 days. For NLRC4 inflammasome activation, peritoneal macrophages were treated with LFn-Fla or LFn-Fla 3A with PA for the indicated times. For NLRP1b inflammasome activation, the cells (J774, RAW264.7, or RAW-asc) were cultured with LF (2 μg/ml; no. 172C, List Biological Labs) together with PA (2 μg/ml; no. 171E, List Biological Labs) for the indicated times. LPS (L2018, Sigma-Aldrich)–primed J774 or RAW-asc cells were stimulated with 10 μM nigericin (tlrl-nig-5, InvivoGen) for NLRP3 inflammasome activation and transfected with Poly (dA:dT) (2 μg/ml; tlrl-patn-1, InvivoGen) for AIM2 inflammasome activation by using Lipofectamine LTX with Plus Reagent (15338100, Thermo Fisher Scientific). Human THP-1 cells were treated with 100 nM phorbol 12-myristate 13-acetate (PMA) for 3 hours and then cultured overnight without PMA before stimulation. Peritoneal macrophages and THP1 cells were cultured in RPMI 1640 medium supplemented with 10% fetal bovine serum (FBS; SH30071.03, HyClone), penicillin (100 units/ml), and streptomycin (100 μg/ml). The J774, RAW264.7, and RAW-asc cells were cultured in Dulbecco's modified Eagle's medium supplemented with 10% FBS (10099-141, Gibco), penicillin (100 units/ml), and streptomycin (100 μg/ml).

Immunoblot analysis

Cell lysates and culture supernatants were collected by adding 5× sample buffer [50% glycerol, 10% SDS, 5% 2-mercaptoethanol, 0.02% bromophenol blue, and 250 mM (pH 6.8) tris-HCl] for immunoblot analysis. Proteins were separated by 10 to 15% polyacrylamide gels, followed by electrophoretic transfer to polyvinylidene difluoride membranes (IPVH00010, Millipore). The membrane was then blocked by incubation with 5% bovine serum albumin before being incubated with primary antibodies. Antibodies used include caspase-1 (clone 4B4) [a gift from V. M. Dixit (Genetech, USA)], caspase-3 (9662, Cell Signaling Technology), pro–caspase-8 (4790, Cell Signaling Technology), cleaved caspase-8 (9429, Cell Signaling Technology), Apaf1 (8723, Cell Signaling Technology), caspase-9 (9508, Cell Signaling Technology), GSDMD (ab209845, Abcam), ASC (67824, Cell Signaling Technology), GSDME (ab215191, Abcam), and glyceraldehyde-3-phosphate dehydrogenase (AC002, ABclonal).

Cross-linking of ASC oligomers

To detect ASC oligomerization, cells were lysed with 0.5% Triton X-100 lysis buffer and then centrifuged at 6000*g* at 4°C for 15 min. Supernatants were transferred to new tubes (lysates). The pellets were washed twice with tris-buffered saline and then cross-linked for 45 min at 37°C by disuccinimidyl suberate (2 mM; Thermo Fisher Scientific). The cross-linked pellets were centrifuged at 6000*g* for 15 min, dissolved in SDS sample buffer, and subjected to Western blot.

Confocal microscopy

Mouse ASC was detected by using a rabbit-ASC monoclonal antibody (67824, Cell Signaling Technology) followed by Alexa Fluor 488 goat anti-rabbit immunoglobulin G (H + L) antibody (A11034, Invitrogen). The nuclei were stained by Hoechst (H1399, Invitrogen). The stained cells were examined under Axio Observer (Zeiss, Germany) at room temperature. Images were acquired and analyzed using Zen2012 software (Zeiss, Germany).

LDH and cell viability assay

Cytotoxicity was determined by measuring LDH activity in the culture medium using the Cytotoxicity LDH Assay Kit-WST (CK12-500-wells, Dojindo). For peritoneal lavage detection, 50 μl of assay reagent was added to peritoneal lavages of an equal volume isolated from mice by using 1 ml of PBS. The CellTiter-Glo Luminescent Cell Viability Assay Kit was used to determine the number of viable cells according to the manufacturer's instructions (G7571, Promega).

Measurement of caspase-1, caspase-3/7, and caspase-8 activities

Caspase-1, caspase-3/7, and caspase-8 activities were determined by using a caspase-Glo 1 (G9951, Promega), caspase-Glo 3/7 (G8092, Promega), or caspase-8 assay kit (G8202, Promega) according to the manufacturer's instructions. Cells were seeded in 96-well plate with white wall (Nunc). After treatment, an equal volume of caspase-Glo 1, caspase-Glo 3/7, or caspase-8 reagent was added to the cell culture medium and shaken for 30 min. Luminescent recording was performed with POLAR star Omega (BMG Labtech). For peritoneal lavage detection, 50 μl of assay reagent was added to peritoneal lavages of an equal volume isolated from mice by using 1 ml of PBS.

Enzyme-linked immunosorbent assay

Mouse TNF (88-7324-88, eBioscence), IL-1β (88-7013-88, eBioscence), and IL-6 (88-7064-77, eBioscence) were measured by enzyme-linked immunosorbent assay according to the manufacturer's instructions.

Statistical analysis

GraphPad Prism 5.0 software (GraphPad Software Inc) was used for data analysis. Data are shown as means ± SE. Survival curves were compared using log rank test (Mantel-Cox). P value less than 0.05 was considered to be statistically significant. $^{***}P < 0.001$ versus WT group and $^{*}P < 0.05$ versus WT FlaTox group.

SUPPLEMENTARY MATERIALS

Supplementary material for this article is available at https://science.org/doi/10.1126/sciadv.abi9471

View/request a protocol for this paper from *Bio-protocol*.

REFERENCES AND NOTES

1. K. Schroder, J. Tschopp, The inflammasomes. *Cell* **140**, 821–832 (2010).
2. N. Kayagaki, S. Warming, M. Lamkanfi, L. V. Walle, S. Louie, J. Dong, K. Newton, Y. Qu, J. Liu, S. Heldens, J. Zhang, W. P. Lee, M. Roose-Girma, V. M. Dixit, Non-canonical inflammasome activation targets caspase-11. *Nature* **479**, 117–121 (2011).
3. J. J. Shi, Y. Zhao, Y. Wang, W. Gao, J. Ding, P. Li, L. Hu, F. Shao, Inflammatory caspases are innate immune receptors for intracellular LPS. *Nature* **514**, 187–192 (2014).
4. S. Y. Wang, M. Miura, Y. K. Jung, H. Zhu, E. Li, J. Yuan, Murine caspase-11, an ICE-interacting protease, is essential for the activation of ICE. *Cell* **92**, 501–509 (1998).
5. P. Li, H. Allen, S. Banerjee, S. Franklin, L. Herzog, C. Johnston, J. McDowell, M. Paskind, L. Rodman, J. Salfeld, E. Towne, D. Tracey, S. Wardwell, F. Y. Wei, W. Wong, R. Kamen, T. Seshadri, Mice deficient in IL-1β-converting enzyme are defective in production of mature IL-1β and resistant to endotoxic shock. *Cell* **80**, 401–411 (1995).
6. J. J. Shi, W. Q. Gao, F. Shao, Pyroptosis: Gasdermin-mediated programmed necrotic cell death. *Trends Biochem. Sci.* **42**, 245–254 (2017).
7. W. T. He, H. Wan, L. Hu, P. Chen, X. Wang, Z. Huang, Z. H. Yang, C. Q. Zhong, J. Han, Gasdermin D is an executor of pyroptosis and required for interleukin-1β secretion. *Cell Res.* **25**, 1285–1298 (2015).
8. N. Kayagaki, I. B. Stowe, B. L. Lee, K. O'Rourke, K. Anderson, S. Warming, T. Cuellar, B. Haley, M. Roose-Girma, Q. T. Phung, P. S. Liu, J. R. Lill, H. Li, J. Wu, S. Kummerfeld, J. Zhang, W. P. Lee, S. J. Snipas, G. S. Salvesen, L. X. Morris, L. Fitzgerald, Y. Zhang, E. M. Bertram, C. C. Goodnow, V. M. Dixit, Caspase-11 cleaves gasdermin D for non-canonical inflammasome signalling. *Nature* **526**, 666–671 (2015).
9. J. J. Shi, Y. Zhao, K. Wang, X. Shi, Y. Wang, H. Huang, Y. Zhuang, T. Cai, F. Wang, F. Shao, Cleavage of GSDMD by inflammatory caspases determines pyroptotic cell death. *Nature* **526**, 660–665 (2015).
10. X. Chen, W. T. He, L. Hu, J. Li, Y. Fang, X. Wang, X. Xu, Z. Wang, K. Huang, J. Han, Pyroptosis is driven by non-selective gasdermin-D pore and its morphology is different from MLKL channel-mediated necroptosis. *Cell Res.* **26**, 1007–1020 (2016).
11. J. J. Ding, K. Wang, W. Liu, Y. She, Q. Sun, J. Shi, H. Sun, D.-C. Wang, F. Shao, Pore-forming activity and structural autoinhibition of the gasdermin family. *Nature* **535**, 111–116 (2016).
12. T. Vanden Berghe, D. Demon, P. Bogaert, B. Vandendriessche, A. Goethals, B. Depuydt, M. Vuylsteke, R. Roelandt, E. Van Wonterghem, J. Vandenbroecke, S. M. Choi, E. Meyer, S. Krautwald, W. Declercq, N. Takahashi, A. Cauwels, P. Vandenabeele, Simultaneous targeting of IL-1 and IL-18 is required for protection against inflammatory and septic shock. *Am. J. Respir. Crit. Care Med.* **189**, 282–291 (2014).
13. J. von Moltke, N. J. Trinidad, M. Moayeri, A. F. Kintzer, S. B. Wang, N. van Rooijen, C. R. Brown, B. A. Krantz, S. H. Leppla, K. Gronert, R. E. Vance, Rapid induction of inflammatory lipid mediators by the inflammasome in vivo. *Nature* **490**, 107–111 (2012).
14. E. A. Miao, I. A. Leaf, P. M. Treuting, D. P. Mao, M. Dors, A. Sarkar, S. E. Warren, M. D. Wewers, A. Aderem, Caspase-1-induced pyroptosis is an innate immune effector mechanism against intracellular bacteria. *Nat. Immunol.* **11**, 1136–1142 (2010).
15. M. Doerflinger, Y. Deng, P. Whitney, R. Salvamoser, S. Engel, A. J. Kueh, L. Tai, A. Bachem, E. Gressier, N. D. Geoghegan, S. Wilcox, K. L. Rogers, A. L. Garnham, M. A. Dengler, S. M. Bader, G. Ebert, J. S. Pearson, D. de Nardo, N. Wang, C. Yang, M. Pereira, C. E. Bryant, R. A. Strugnell, J. E. Vince, M. Pellegrini, A. Strasser, S. Bedoui, M. J. Herold, Flexible usage and interconnectivity of diverse cell death pathways protect against intracellular infection. *Immunity* **53**, 533–547.e7 (2020).

16. Y. Zhao, J. Shi, X. Shi, Y. Wang, F. Wang, F. Shao, Genetic functions of the NAIP family of inflammasome receptors for bacterial ligands in mice. *J. Exp. Med.* **213**, 647–656 (2016).
17. I. Rauch, K. A. Deets, D. X. Ji, J. von Moltke, J. L. Tenthorey, A. Y. Lee, N. H. Philip, J. S. Ayres, I. E. Brodsky, K. Gronert, R. E. Vance, NAIP-NLRC4 inflammasomes coordinate intestinal epithelial cell expulsion with eicosanoid and IL-18 release via activation of caspase-1 and -8. *Immunity* **46**, 649–659 (2017).
18. L. Franchi, Role of inflammasomes in *Salmonella* infection. *Front. Microbiol.* **2**, 8 (2011).
19. M. Lamkanfi, V. M. Dixit, Mechanisms and functions of inflammasomes. *Cell* **157**, 1013–1022 (2014).
20. V. Sagulenko, S. J. Thygesen, D. P. Sester, A. Idris, J. A. Cridland, P. R. Vajjhala, T. L. Roberts, K. Schroder, J. E. Vince, J. M. Hill, J. Silke, K. J. Stacey, AIM2 and NLRP3 inflammasomes activate both apoptotic and pyroptotic death pathways via ASC. *Cell Death Differ.* **20**, 1149–1160 (2013).
21. R. Pierini, C. Juruj, M. Perret, C. L. Jones, P. Mangeot, D. S. Weiss, T. Henry, AIM2/ASC triggers caspase-8-dependent apoptosis in Francisella-infected caspase-1-deficient macrophages. *Cell Death Differ.* **19**, 1709–1721 (2012).
22. P. R. Vajjhala, A. Lu, D. L. Brown, S. W. Pang, V. Sagulenko, D. P. Sester, S. O. Cridland, J. M. Hill, K. Schroder, J. L. Stow, H. Wu, K. J. Stacey, The inflammasome adaptor ASC induces procaspase-8 death effector domain filaments. *J. Biol. Chem.* **290**, 29217–29230 (2015).
23. N. Van Opdenbosch, H. Van Gorp, M. Verdonckt, P. H. V. Saavedra, N. M. de Vasconcelos, A. Gonçalves, L. V. Walle, D. Demon, M. Matusiak, F. Van Hauwermeiren, J. D'Hont, T. Hochepied, S. Krautwald, T.-D. Kanneganti, M. Lamkanfi, Caspase-1 engagement and TLR-induced c-FLIP expression suppress ASC/caspase-8-dependent apoptosis by inflammasome sensors NLRP1b and NLRC4. *Cell Rep.* **21**, 3427–3444 (2017).
24. Y. Zhao, J. Yang, J. Shi, Y. N. Gong, Q. Lu, H. Xu, L. Liu, F. Shao, The NLRC4 inflammasome receptors for bacterial flagellin and type III secretion apparatus. *Nature* **477**, 596–600 (2011).
25. F. Hayashi, K. D. Smith, A. Ozinsky, T. R. Hawn, E. C. Yi, D. R. Goodlett, J. K. Eng, S. Akira, D. M. Underhill, A. Aderem, The innate immune response to bacterial flagellin is mediated by Toll-like receptor 5. *Nature* **410**, 1099–1103 (2001).
26. Y. Wang, W. Gao, X. Shi, J. Ding, W. Liu, H. He, K. Wang, F. Shao, Chemotherapy drugs induce pyroptosis through caspase-3 cleavage of a gasdermin. *Nature* **547**, 99–103 (2017).
27. C. Rogers, T. Fernandes-Alnemri, L. Mayes, D. Alnemri, G. Cingolani, E. S. Alnemri, Cleavage of DFNA5 by caspase-3 during apoptosis mediates progression to secondary necrotic/pyroptotic cell death. *Nat. Commun.* **8**, 14128 (2017).
28. K. S. Schneider, C. J. Groß, R. F. Dreier, B. S. Saller, R. Mishra, O. Gorka, R. Heilig, E. Meunier, M. S. Dick, T. Ćiković, J. Sodenkamp, G. Médard, R. Naumann, J. Ruland, B. Kuster, P. Broz, O. Groß, The inflammasome drives GSDMD-independent secondary pyroptosis and IL-1 release in the absence of caspase-1 protease activity. *Cell Rep.* **21**, 3846–3859 (2017).
29. S. Mariathasan, K. Newton, D. M. Monack, D. Vucic, D. M. French, W. P. Lee, M. Roose-Girma, S. Erickson, V. M. Dixit, Differential activation of the inflammasome by caspase-1 adaptors ASC and Ipaf. *Nature* **430**, 213–218 (2004).
30. K. W. Chen, C. J. Groß, F. V. Sotomayor, K. J. Stacey, J. Tschopp, M. J. Sweet, K. Schroder, The neutrophil NLRC4 inflammasome selectively promotes IL-1β maturation without pyroptosis during acute Salmonella challenge. *Cell Rep.* **8**, 570–582 (2014).
31. J. L. Levinsohn, Z. L. Newman, K. A. Hellmich, R. Fattah, M. A. Getz, S. Liu, I. Sastalla, S. H. Leppla, M. Moayeri, Anthrax lethal factor cleavage of Nlrp1 Is required for activation of the inflammasome. *PLOS Pathog.* **8**, e1002638 (2012).
32. J. Chavarria-Smith, R. E. Vance, Direct proteolytic cleavage of NLRP1B Is necessary and sufficient for inflammasome activation by anthrax lethal factor. *PLOS Pathog.* **9**, e1003452 (2013).
33. A. Sandstrom, P. S. Mitchell, L. Goers, E. W. Mu, C. F. Lesser, R. E. Vance, Functional degradation: A mechanism of NLRP1 inflammasome activation by diverse pathogen enzymes. *Science* **364**, eaau1330 (2019).
34. E. D. Boyden, W. F. Dietrich, Nalp1b controls mouse macrophage susceptibility to anthrax lethal toxin. *Nat. Genet.* **38**, 240–244 (2006).
35. A. J. Chui, M. C. Okondo, S. D. Rao, K. Gai, A. R. Griswold, D. C. Johnson, D. P. Ball, C. Y. Taabazuing, E. L. Orth, B. A. Vittimberga, D. A. Bachovchin, N-terminal degradation activates the NLRP1B inflammasome. *Science* **364**, 82–85 (2019).
36. W. S. Bollen, B. M. Gunn, H. Mo, M. K. Lay, R. Curtiss 3rd, Presence of wild-type and attenuated Salmonella enterica strains in brain tissues following inoculation of mice by different routes. *Infect. Immun.* **76**, 3268–3272 (2008).
37. S. M. Man, L. J. Hopkins, E. Nugent, S. Cox, I. M. Gluck, P. Tourlomousis, J. A. Wright, P. Cicuta, T. P. Monie, C. E. Bryant, Inflammasome activation causes dual recruitment of NLRC4 and NLRP3 to the same macromolecular complex. *Proc. Natl. Acad. Sci. U.S.A.* **111**, 7403–7408 (2014).
38. S. M. Crowley, X. Han, J. M. Allaire, M. Stahl, I. Rauch, L. A. Knodler, B. A. Vallance, Intestinal restriction of *Salmonella* Typhimurium requires caspase-1 and caspase-11 epithelial intrinsic inflammasomes. *PLOS Pathog.* **16**, e1008498 (2020).
39. M. Lara-Tejero, F. S. Sutterwala, Y. Ogura, E. P. Grant, J. Bertin, A. J. Coyle, R. A. Flavell, J. E. Galán, Role of the caspase-1 inflammasome in Salmonella typhimurium pathogenesis. *J. Exp. Med.* **203**, 1407–1412 (2006).
40. S. Felgner, D. Kocijancic, M. Frahm, U. Heise, M. Rohde, K. Zimmermann, C. Falk, M. Erhardt, S. Weiss, Engineered *Salmonella* enterica serovar Typhimurium overcomes limitations of anti-bacterial immunity in bacteria-mediated tumor therapy. *Oncoimmunology* **7**, e1382791 (2018).
41. S. A. Johnson, M. J. Ormsby, D. M. Wall, Draft genome sequence of the tumor-targeting salmonella enterica serovar typhimurium strain SL7207. *Genome Announc.* **5**, e01591-16 (2017).
42. M. Miura, H. Zhu, R. Rotello, E. A. Hartwieg, J. Y. Yuan, Induction of apoptosis in fibroblasts by IL-1β-converting enzyme, a mammalian homolog of the C. elegans cell death gene Ced-3. *Cell* **75**, 653–660 (1993).
43. X. Jiang, X. Wang, Cytochrome c promotes caspase-9 activation by inducing nucleotide binding to Apaf-1. *J. Biol. Chem.* **275**, 31199–31203 (2000).
44. H. L. Li, H. Zhu, C. J. Xu, J. Y. Yuan, Cleavage of BID by caspase 8 mediates the mitochondrial damage in the Fas pathway of apoptosis. *Cell* **94**, 491–501 (1998).
45. X. Luo, I. Budihardjo, H. Zou, C. Slaughter, X. D. Wang, Bid, a Bcl2 interacting protein, mediates cytochrome c release from mitochondria in response to activation of cell surface death receptors. *Cell* **94**, 481–490 (1998).
46. K. Tsuchiya, S. Nakajima, S. Hosojima, D. T. Nguyen, T. Hattori, T. M. Le, O. Hori, M. R. Mahib, Y. Yamaguchi, M. Miura, T. Kinoshita, H. Kushiyama, M. Sakurai, T. Shiroishi, T. Suda, Caspase-1 initiates apoptosis in the absence of gasdermin D. *Nat. Commun.* **10**, 2091 (2019).
47. S. M. Comb, P. K. Chan, A. Guinot, H. Hartmannsdottir, S. Jenni, M. P. Dobay, J.-P. Bourquin, B. C. Bornhauser, Efficient apoptosis requires feedback amplification of upstream apoptotic signals by effector caspase-3 or −7. *Sci. Adv.* **5**, eaau9433 (2019).
48. B. L. Lee, K. M. Mirrashidi, I. B. Stowe, S. K. Kummerfeld, C. Watanabe, B. Haley, T. L. Cuellar, M. Reichelt, N. Kayagaki, ASC- and caspase-8-dependent apoptotic pathway diverges from the NLRC4 inflammasome in macrophages. *Sci. Rep.* **8**, 3788 (2018).
49. D. P. A. Mascarenhas, D. M. Cerqueira, M. S. F. Pereira, F. V. S. Castanheira, T. D. Fernandes, G. Z. Manin, L. D. Cunha, D. S. Zamboni, Inhibition of caspase-1 or gasdermin-D enable caspase-8 activation in the Naip5/NLRC4/ASC inflammasome. *PLOS Pathog.* **13**, e1006502 (2017).
50. C. Y. Taabazuing, M. C. Okondo, D. A. Bachovchin, Pyroptosis and apoptosis pathways engage in bidirectional crosstalk in monocytes and macrophages. *Cell. Chem. Biol.* **24**, 507–514.e4 (2017).
51. P. Orning, D. Weng, K. Starheim, D. Ratner, Z. Best, B. Lee, A. Brooks, S. Xia, H. Wu, M. A. Kelliher, S. B. Berger, P. J. Gough, J. Bertin, M. M. Proulx, J. D. Goguen, N. Kayagaki, K. A. Fitzgerald, E. Lien, Pathogen blockade of TAK1 triggers caspase-8-dependent cleavage of gasdermin D and cell death. *Science* **362**, 1064–1069 (2018).
52. H. Bantel, K. Schulze-Osthoff, Cell death in sepsis: A matter of how, when, and where. *Crit. Care* **13**, 173 (2009).
53. S. Hofer, T. Brenner, C. Bopp, J. Steppan, C. Lichtenstern, J. Weitz, T. Bruckner, E. Martin, U. Hoffmann, M. A. Weigand, Cell death serum biomarkers are early predictors for survival in severe septic patients with hepatic dysfunction. *Crit. Care* **13**, R93 (2009).

Acknowledgments: We thank V. M. Dixit for caspase-1 antibody (clone 4B4), R. E. Vance for plasmids of pET15b LFn-Fla and pET15b LFn-Fla 3A, and Z. Pan for *Salmonella* SL7207 (ΔaroA). We thank L. Zhou (Xiamen University) for proofreading the manuscript. We thank the Laboratory Animal Center of Xiamen University for technical support. **Funding:** This work was supported by the National Natural Science Foundation of China (81788101 and 81630042 to J.H. and 31701205 to P.Z.), the National Scientific and Technological Major Project (2017ZX10202203-003 to J.H.), the National Key R&D program (2020YFA0803500 to J.H.), the 111 Project (B12001 to J.H.), the CAMS Innovation Found for Medical Science (CIFMS) (2019-I2M-5-062 to J.H.), and the U.S. National Institute of Health grant (5U19 AI100627-08 to R.J.U.). **Author contributions:** P.Z., Y.L., L.H., K.H., M.H., Y.W., and X.F., carried out experimental work. P.Z, Y.L., R.J.U., and J.H. designed experiments and interpreted the data. P.Z. and J.H. wrote the manuscript. J.H. conceived and supervised the study. The authors reviewed and approved the final version of the paper. **Competing interests:** The authors declare that they have no competing interests. **Data and materials availability:** All data needed to evaluate the conclusions in the paper are present in the paper and/or the Supplementary Materials.

Submitted 10 April 2021
Accepted 31 August 2021
Published 22 October 2021
10.1126/sciadv.abi9471

Citation: P. Zhang, Y. Liu, L. Hu, K. Huang, M. Hong, Y. Wang, X. Fan, R. J. Ulevitch, J. Han, NLRC4 inflammasome–dependent cell death occurs by a complementary series of three death pathways and determines lethality in mice. *Sci. Adv.* **7**, eabi9471 (2021).